POSITRON EMISSION TOMOGRAPHY SYSTEMS BASED ON IONIZATION-ACTIVATED ORGANIC FLUOR MOLECULES

BACKGROUND

[0001] Conventional positron-emission tomography (PET) has unique capabilities in diagnostics. However, its use is limited by the large radiation dose to the patient, limited resolution, the cost of high-density crystal scintillators, and in many configurations a complicated mechanical construction.

[0002] Commercial PET detectors use high-density crystals as scintillators to lessen blurring due to the non-point-like nature of energy deposition by gamma-rays in the crystal. The crystal scintillators are expensive and the high cost has resulted in wide-spread use of scanner designs with reduced geometrical coverage. This forces a longer exposure during which a small-solid-angle scanner moves over the patient in multiple scans, resulting in a larger total radiation dose to the patient. The precision scanner mechanisms are expensive and need to be maintained. The longer exposure time may limit the through-put of the system, increasing the cost-per-patient.

[0003] In current PET detector designs, the spatial resolution on the gamma-ray interaction point is proportional to the size of the crystals. Measuring the distribution of light shared with neighboring crystals allows a resolution in the plane of the crystal array that is a fraction of the crystal size.

[0004] Time-of-flight PET (TOF-PET) supplies information on the position of a positron-electron annihilation along a line-of-response (LOR) by measuring the difference in times of arrival of the gamma-ray pairs generated by the annihilation in two opposing crystals in a detector array. The typical time resolution of commercial TOF-PET scanners is 500 psec, corresponding to a spatial resolution of about 150 mm along the line-of-response (the gamma-gamma axis).

[0005] PET is currently limited in use to large hospitals and for a limited set of patients. For example, hairline fractures, which are common in falls of the elderly, can be difficult to diagnose with X-rays, but are highly visible in a PET scan. However, the preparation and large radiation dose dictate against the prescription of PET in such cases, and the less-effective X-ray diagnostic is instead widely prescribed instead of PET. The large radiation

1

dose also limits the patient population that can be exposed and how often; for example, the use of PET for children is typically recommended only for extreme cases.

SUMMARY

[0006]   Positron emission tomography (PET) and time-of-flight positron emission tomography (TOF-PET) systems and methods for imaging samples using these systems are provided. The PET systems can be used in conventional patient imaging applications. In addition, because the PET systems can operate using low radiation doses and provide high image resolution, they can also be used to open new avenues for diagnosis and treatment. Examples include early detection of immune response to a pathogen, follow-up diagnosis after serological diagnosis of cancer, and real-time monitoring of hadron therapy.

[0007]   One embodiment of a PET system includes a plurality of imaging modules arranged to image a sample, such as a human patient. The imaging modules include: a scintillator compartment containing a scintillating medium comprising one or more fluors and scintillator compartment having an opaque, reflecting, or transparent front face and a transparent back face; a photodetector system comprising one or more photodetectors optically coupled to the scintillator compartment and configured to detect scintillation photons generated in the scintillating medium; and an optical imaging system. The optical imaging system includes: one or more excitation light sources that are optically coupled to the scintillator compartment and configured to direct excitation light onto the scintillating medium; and one or more fluorescence detectors that optically coupled to the scintillator compartment and configured to detect fluorescence generated by the fluors in the scintillating medium.

[0008]   One embodiment of a method for imaging a sample using the PET system of the type described herein includes the steps of: positioning a sample within an imaging volume defined by a plurality of imaging modules, wherein positron-electron annihilation events in the sample generate coincident gamma-ray pairs; detecting scintillation photons generated by the interaction of each gamma-ray of a coincident gamma-ray pair with the scintillating media in two opposing imaging modules to identify an initial lines-of-response for the coincident gamma-ray pair; triggering the excitation light sources to excite fluors in the scintillating medium of each imaging module; and recording fluorescence emitted by the excited fluors to generate an image of energy clusters corresponding to Compton scatters of

the gamma-rays in the scintillation material. The recorded fluorescence can then be used to: identify the energy cluster corresponding to the earliest Compton scatter for both of the gamma-rays; determine the energy, trajectory and direction of the Compton scattered electrons for the earliest Compton scatters for each gamma-ray to identify the location of a first collision between each gamma-ray and an electron in the scintillating medium; and improve the resolution on the line-of-response for the coincident gamma-ray pair, by using the locations of the first collisions as end points for the line-of-response.

[0009]   Other principal features and advantages of the invention will become apparent to those skilled in the art upon review of the following drawings, the detailed description, and the appended claims.

BRIEF DESCRIPTION OF THE DRAWINGS

[0010]   Illustrative embodiments of the invention will hereafter be described with reference to the accompanying drawings, wherein like numerals denote like elements.

[0011]   FIG. 1. An implementation of a modular TOF-PET whole-body scanner based on Switchillators. A sample [1] is located in the center of a cylindrical array of imaging modules. In this example each of the two gamma-rays of a gamma-ray pair enters an imaging module through a front-side mirror acting as the entrance surface. A fast timing photodetector (FT-photodetector) [6] is optically coupled through the back surface of the module. An optics system [8] controls the scanning and focus of twin lasers [7] in the active Switchillator volume [2]. CCD cameras [5] have a wide-angle stereo view of the active Switchillator volume through the backside surface and a passive optical transition volume [3] that is optically matched to the active volume [2].

[0012]   FIG. 2. Plan view of an example implementation of a single imaging module for a cylindrical TOF-PET whole-body scanner such as shown in FIG. 1. The sample is located below the module; the gamma-rays [3] enter the Switchillator volume [4] through a front window [2] and mirror [1]. The CCD cameras [10] and the lasers [9] view the active Switchillator volume [4] through the backside of the Switchillator compartment and the optically matched transition volume [5]. The left-hand panel shows the CCD camera subsystem comprising the cameras [10], the camera optic components [7a] and a reflecting prism [8]. The right-hand panel shows the same module rotated by 90 degrees to display the

twin laser subsystem comprising the lasers [9], the laser optic components [7b] and the reflecting prism [8].

[0013]   FIG. 3. A 3D view of an example implementation of a single imaging module for a cylindrical TOF PET whole-body scanner such as shown in FIG. 1. The sample is located below the module. The gamma-ray encounters in sequence the entrance surface [7] which is mirrored on the inside, the active scintillator volume [1], and the optically matched transition volume that does not contain fluor molecules [2]. The FT-photodetector [4] is optically coupled to the transparent backside surface of the Switchillator compartment. An optics subsystem [3] controls the scanning and focus of twin diode lasers [5] in the active Switchillator volume [1]. The twin diode lasers [5] illuminate the volume [1] through the backside surface around the FT-photodetector.

[0014]   FIG. 4. A Geant4 simulation of a 511 KeV gamma-ray interacting in a hydrocarbon scintillating medium with H:C equal to 1.96 (specifically the scintillator used in the Kamland-Zen neutrino experiment), in an imaging module. (Gando, A., et al. "Search for Majorana neutrinos near the inverted mass hierarchy region with KamLAND-Zen." *Physical review letters* 117.8 (2016): 082503) The gamma-ray path is indicated with a gray line connecting the locations of Compton scatters. The energy deposition at each scatter is color-coded from blue (low energy fraction) to red (high energy fraction).

[0015]   FIG. 5. Right: A view of a pixelated digital-camera image with 1 cm pixels showing energy depositions in the simulation of the 511 KeV gamma-ray of FIG. 4. Left: maps of energy depositions from two different Compton scattered electrons. Top-left: the energy deposition map showing the energy cluster corresponding to the most energetic Compton scatter, with a pixel resolution of 10 μm. Bottom-left: the energy deposition map showing the energy cluster corresponding to the second-most energetic Compton scatter, with a pixel resolution of 1 μm. The intensity of the energy deposition in each pixel is color-coded from blue (low energy fraction) to red (high energy fraction).

[0016]   FIG. 6. The output of a seed-shoulder clustering algorithm applied to the energy cluster shown in the top left panel of FIG. 5, as described in Example 2.

[0017]   FIG. 7. The number of scintillation photons produced by the 511 keV gamma-ray in the Kamland-Zen-like scintillating medium, from a simulation of 10,000 gamma-rays. The number of photons from all Compton scatters is plotted on the right; the photons produced by the most energetic Compton scatter is plotted on the left.

[0018] FIG. 8. Tabulation of the fractional energy deposited by the 511 keV gamma-ray in successive Compton scatters in the Kamland-Zen scintillating medium. The rows correspond to the fraction of 511 keV deposited in each interaction. The columns represent the first through fifth interactions between the gamma-ray and the scintillating medium. The entries are event counts from 10,000 simulated gamma-rays.

[0019] FIG. 9. The longitudinal [Left] and transverse [Right] positions of the brightest interaction between the 511 keV gamma-ray and the scintillating medium in a line-of-response reference frame in the Kamland-Zen hydrocarbon scintillating medium. Ninety percent of the gamma-rays interact within 30 cm of the entrance to the active Switchillator volume.

[0020] FIG. 10. Top: A tabulation of the number of positron-electron annihilation events, out of 10,000 simulated, in which the first interaction of the gamma-ray is the most energetic Compton scatter for both gamma-rays of a coincident pair, the first scatter for one of the two gamma-rays is the most energetic Compton scatter, and the first scatter for neither of the two gamma-rays is the most energetic Compton scatter. These three columns are further subdivided into the cases in which the direction of the recoil electron is correctly reconstructed for both, one, and neither gamma-ray. Bottom: The corresponding plots of the impact parameter (distance of closest approach) of the LOR to the true emission point in the sample. When both first interactions are the most energetic Compton scatter, the impact parameter is predominantly less than 30 μm for a voxel size of 20 μm. If either first interaction is not the most energetic, the median impact parameter is 35 millimeters (35,000 microns), and consequently these events have little impact on resolution and contrast, forming a featureless flat background to true signal.

[0021] FIG. 11. An example LOR drawn between the first Compton scatter in each of two opposing imaging modules, in the case of no gamma-ray scattering in the patient.

[0022] FIG. 12. An example LOR drawn between the first Compton scatter in each of the opposing imaging modules, in the case of in-patient gamma-ray scattering. The Compton scatter is fully-constrained by the Compton 2-body kinematical equations.

[0023] FIG. 13. An example LOR drawn between the first Compton scatter in each of the opposing imaging modules, in the case that gamma-ray scattering in the patient is out of the plane reconstructed in the imaging module of the Compton scattered gamma and the recoil electron.

[0024]   FIG. 14. For one simulated event, the distribution in the time between the arrival of the 511 keV gamma-ray at the front face of an imaging module (t=0) and the arrival of individual scintillation photons at an FT-photodetector on the back surface in the ideal case of a fast scintillator with zero lifetime. Distributions are shown for both the direct and reflected light. This event occurs near the back of the imaging module so that the photon times are near the light-time to cross the module, assumed here to be 300 mm. The gamma-ray travels at the speed of light, c; the photon velocity is lower by a factor of the index of refraction, here taken to be 1.4.

[0025]   FIG. 15. For the same selection criteria as in FIG. 14, the distribution in the time of emission of the photons from the brightest cluster.

[0026]   FIG. 16. Time-of-flight resolution for an on-axis point-source sample, derived from the arrival time of the first photon identified for each of the two brightest clusters. The scintillator is assumed to have the limited Kamland-Zen light yield, but had been chosen for a short lifetime, such that the emission time of the first photon arriving is negligible.

[0027]   FIG. 17. The specifications (center) and figures (left and right) of the commercially available Standard Jaszczak Phantom used to test and calibrate PET and SPECT scanners. The phantom contains cylinders filled with a radioactive tracer solution in a tight-fitting volume filled with lower tracer concentration. The spheres in the photograph were not simulated.

[0028]   FIG.18. Left: Generated annihilation coordinates from a simulation of the Standard Jaszczack Phantom(TM) described in FIG. 17, but with two cylinders of 10 cm length and the same diameter, each containing a `background' loading of 100 Bq/ml of 18F appended to the top and bottom faces of the standard phantom. Center: The filtered backprojection of the left panel, with a pixel size of 1 mm. Right: The center panel image smoothed by a Gaussian filter of 2 mm. The hot rods are loaded with 300 Bq/ml of 18F, while the background is loaded with 100 Bq/ml of 18F. The efficiency of reconstructing the LOR to within a sigma of 20 μm is assumed to be 10%; the detector is assumed to have a radius of 30 cm and an axial length of 30 cm, corresponding to the length of a single module; the exposure is set to 10 minutes.

DETAILED DESCRIPTION

[0029] High-spatial resolution PET systems are provided. The PET systems are constructed from imaging modules that include: a scintillating medium that contains an ionization-activated fluorescent substance, such organic fluor molecules; an optical imaging system; and a fast-timing (FT) photodetector system. The scintillation medium containing the fluorescent substance is referred to as a Switchillator. Using the PET systems, the path of a gamma-ray through the scintillation medium can be analyzed in detail and accurately reconstructed to provide improved PET imaging of the source of ionizing radiation, such as gamma-rays. The PET systems described here can be TOF- PET systems. However, the PET systems can also be used with non-PET-TOF systems.

[0030] The PET systems can be used to study a gamma-ray emitting sample. For most applications, the gamma-rays will be emitted from the sample as a coincident gamma-ray pair that result from a positron-electron annihilation event in the sample, and the two coincident gamma-rays of the pair will be detected by opposing imaging modules. A line connecting the locations in the imaging modules at which the two gamma-rays are detected, referred to as a line-of-response (LOR), together with the arrival times of the two gamma-rays can be used to identify the location of the gamma-ray source in the sample.

[0031] When a gamma-ray enters a Switchillator in an imaging module, it undergoes a series of successive scatters (also referred to scattering events) at discrete interaction locations. Through these interactions, the gamma-ray loses its energy to the scintillating medium. The scatters include Compton scatters (also referred to as Compton scattering events) in which the gamma-ray collides with an electron. The energy and angle of the scattered electron and gamma-ray in Compton scattering are constrained by Compton kinematics. At each scatter, prompt scintillation light is emitted and this prompt scintillation light is detected by the FT-photodetector system, which provides a coincident trigger for the optical imaging system. If the FT-photodetector system is a TOF system, the arrival times of the prompt scintillation photons are also used to determine the location of the source of the coincident gamma-rays along the LOR.

[0032] At each Compton scatter, the Compton scattered electron (also referred to as a recoil electron) deposits ionization energy along its track as it moves through the Switchillator. The deposited ionization energy activates the fluor molecules in the vicinity of

the ionization and the optical imaging subsystem is used to repeatedly excite the activated fluors and image the resulting fluorescence in order to reconstruct the recoil electron track.

[0033]   From the distribution pattern and fluorescence intensity of the activated fluors, the earliest Compton scatter can be identified, the path of the gamma-ray through the Switchillator can be reconstructed, the starting point of the track of a Compton electron can be identified, and the energy deposited along the path of the gamma-ray and the tracks of the Compton electrons can be determined. This information can be used to improve the imaging of a gamma-ray source by identifying, with high resolution, the end-points of an LOR, which corresponds to the starting point of the track of the first Compton scattered electron in the Switchillator. By way of illustration, the precision of the end points of a LOR for a gamma-ray pair can be improved by identifying, on a statistical basis, the earliest detectable interaction point of a gamma-ray in the Switchillator with a resolution of 100 μm or better, including resolutions of 20 μm or better. The inherent high resolution of the technique allows a significant reduction in radiation dose for a patient relative to conventional PET imaging systems.

[0034]   The imaging of the gamma-ray source can be further improved by identifying and rejecting background signal generated by coincident gamma-rays that have scattered in the sample prior to entering an imaging module or by other background signal-generating events.

[0035]   The activated fluor molecules along the ionization path of a Compton electron are excited and imaged with high-resolution by the optical imaging system, which includes controllable excitation light sources and fluorescence detectors. The high-resolution images provide measurements of the energies and positions of gamma-ray Compton scatters using one or more cycles of fluor excitation and imaging. The optical imaging system can resolve each of the Compton scatters into an energy cluster and the path of the gamma-ray in the Switchillator, including its earliest scatter, can be reconstructed, on a statistical basis, from the clusters. In particular, the following information about can be reconstructed: the location and magnitude of the energy transferred to the fluor molecules; the directions of the scattered gamma-rays and Compton electrons; and the angular relations among the energy clusters associated with the Compton scatters, which are kinematically constrained by the Compton scattering equation. The angular relations among the energy clusters also provide information that can be used to reject background signal generated by gamma-rays that have undergone in-patient scattering.

[0036] The images obtained by the optical imaging system are digitally recorded, enabling the use of advanced algorithms and techniques to determine the topology and number of activated fluor molecules for improved gamma-ray energy and annihilation location resolution, and the rejection of background signal due to in-patient scattering or other background sources.

PET SYSTEM COMPONENTS

[0037] An embodiment of a Switchillator PET system, in this case a modular whole-body TOF-PET scanner, is shown schematically in FIG. 1. The system includes a plurality of imaging modules arranged around a sample (**1**), here a human patient. Although FIG. 1 shows a PET system implemented in a whole-body TOF-PET system, it should be understood that the PET systems need not be part of a whole-body TOF-PET system.

[0038] The PET system may include a sample holder configured to position the sample (**1**) centrally within the imaging volume defined by the imaging modules. In some embodiments, the sample holder is a horizontal platform, such as a table or bed, or a vertical surface against which the sample is placed. Samples to be imaged with PET systems include humans, other animals, and materials.

[0039] For whole-body imaging, the imaging modules may be arranged in a cylindrical geometry around the sample as in a conventional PET detector as illustrated in FIG. 1, or arranged in a moveable rectangular geometry for patient comfort, as described in U.S. patent number 10,132,942, or arranged in a custom geometry for specialized applications. Alternatively, multi-module arrays of the modules can be configured to optimize for differing body sizes and mobility issues. For specialized imaging of smaller samples, such as the brain or extremities, or for example, small animal imaging, application-specific modules can be in a suitably-designed fixed or configurable geometry.

[0040] Plan and three-dimensional views of an exemplary imaging module are shown in FIG. 2 and FIG. 3 respectively. Each imaging module includes a Switchillator compartment containing a fluor-containing scintillating medium. The entire volume of the scintillating medium may include the fluor molecules, or the volume of scintillating medium may include a sub-volume [4] that includes fluor molecules (referred to here as an active volume) and a sub-volume that does not include the fluor molecules [5]. Gamma-rays from positron-electron annihilations in the sample enter the active volume of the scintillating medium through the imaging module surface facing the sample (front surface).

[0041]   Each imaging module has an optical imaging system that includes at least one light source for exciting activated fluor molecules and at least one fluorescence detector for detecting fluorescence emitted by the excited fluor molecules. The imaging modules may further include optical components, electronic circuitry, and data acquisition and analysis systems for generating and displaying digital images. The example implementation of an optical imaging system shown in FIGS. 2 and 3 incorporates dual laser diodes [9a] [9b] as excitation light sources and dual CCD digital cameras [10a] [10b] as fluorescence detectors. The light sources and fluorescence detectors are optically coupled to the scintillator compartment and the Switchillator contained therein, meaning that the light sources are positioned such that light from the light sources can be directed onto the Switchillator, either directly or with the use of an optics system, and that the fluorescence detectors are positioned such that fluorescence emitted by the fluors in the Switchillator can be imaged by the fluorescence detectors, either directly or with the use of an optics system. In the embodiment of FIGS. 2 and 3, the laser diodes and CCD cameras are mounted on the back surface of the Switchillator compartment and the excitation light provided by the twin diode lasers is steered and focused in the horizontal and vertical planes by an optics system composed of controllable mirrors and lenses to provide wide-angle stereo coverage of the entire Switchillator volume. The cameras can also be steered and focused in the horizontal and vertical planes by an optics system composed of controllable mirrors and lenses to provide wide-angle stereo viewing of the entire Switchillator volume.

[0042]   To facilitate full coverage with wide-angle stereo viewing, an optical transition region [5] may be employed between the active Switchillator volume [4] and the back face of the Switchillator compartment. In FIGS. 2 and 3 the transition region is a passive volume containing a transparent fluor-free liquid having an index of refraction that matches the index of refraction of the Switchillator. Alternative geometries may include more sophisticated optical interfaces and optical components.

[0043]   The optical imaging system may further include electronic controls and readout systems and optical components such as mirrors, lenses, prisms, apertures, and/or baffles that allow the beam of excitation light to be shaped, focused, pulsed, and/or scanned over the active Switchillator volume, and to synchronize the beam of excitation light with the fluorescence detectors.

[0044] As shown in FIGS. 2 and 3, a FT-photodetector system that includes a fast-timing photodetector for detecting the initial scintillation light produced by the gamma-ray interaction with the Switchillator also may be also mounted on the back of the Switchillator compartment. The FT-photodetector system may also include electronic controls and readout systems and optical components such as mirrors, lenses, prisms, apertures, and/or baffles. The difference between the calculated times-of-arrival of the gamma-rays of a coincident pair by the FT-photodetector systems of two imaging modules is used to calculate the position of the annihilation event in the sample being imaged along an LOR with an associated uncertainty distribution. In this example implementation, the internal surface of the Switchillator compartment front face has been made reflective to roughly locate energy depositions (scatters) and to improve the arrival time resolution by measuring the difference in scintillation light transit times to the front and back surfaces of the Switchillator compartment.

[0045] In addition to measuring the arrival times of prompt scintillation photons, the FT-photodetector system provides a coincidence trigger for the optical imaging system to initiate a sequence of repeated fluor excitation and fluorescence imaging cycles. If the scintillating medium is a low-density material that enables the resolution of the timing and location of energy depositions associated with discrete Compton scatters, the fast photodetectors can also provide preliminary information about the locations of the energy clusters associated with the Compton scatters in the Switchillator for optical imaging. Such low-density scintillator materials are described in U.S. patent number 10,132,942. Conversely, the time-ordered map of energy clusters and the gamma-ray trajectory reconstructed using the Switchillator can be used to refine the timing and location information from the TOF photodetector system to further refine the LOR end point identification and probability distribution for an annihilation event along the LOR.

[0046] Candidates for the photodetectors used in the FT-photodetector system include, but are not limited to, solid-state photodetectors such as silicon photomultipliers and vacuum-based photomultiplier tubes (PMTs), including MCP-PMTs. In the example implementation of FIGS. 2 and 3, a large-area flat-panel MCP-PMT such as an LAPPD is mounted on the back surface of the Switchillator compartment, and the front surface of the Switchillator is mirrored to be reflective.

[0047] In the example imaging module of FIGS. 2 and 3, electronics used to support control, data acquisition, calibration, and local data analysis, including a complete imaging of the gamma-ray trajectory in the Switchillator, also can be mounted on the back surface of the Switchillator compartment.

SWITCHILLATOR COMPOSITION

[0048] The Switchillator is a transparent material that comprises two components: a first component that absorbs ionizing energy from a gamma-ray and emits scintillation light, typically visible or ultraviolet light; and the fluor molecules that are activated by the deposited ionizing energy and excited by the excitation light sources. The component of the scintillating medium that absorbs ionizing radiation from the gamma-ray and emit prompt scintillation light can also be considered a type of fluor, but is distinguishable from the fluor molecules that are imaged using the optical imaging system. Because the scintillation light emitting fluors ("scintillation fluors") and the fluor molecules imaged by the optical imaging system ("Switchillator fluors") are distinct, the scintillation fluors can be chosen to optimize speed and yield for TOF resolution independent from the choice of the Switchillator fluors.

[0049] Examples of diarylthene Switchillators fluors that can be used in the PET systems are diaryethenes, as described in Kakishi Uno et al. *Journal of the American Chemical Society* 133.34 (2011), pp. 13558–13564; Masahiro Irie et al., *Bulletin of the Chemical Society of Japan* 91.2 (2017), pp. 237–250; Dojin Kim et al., *Advanced Functional Materials* 28.7 (2018), p. 1706213; and Ryota Kashihara et al., *Journal of the American Chemical Society* 139.46 (2017), pp. 16498–16501.

[0050] The scintillating medium can be a solid crystal, gas, or liquid, where the term liquid includes viscous fluids, such as gels. Water-based and organic solvent-based liquid scintillators can be used. In the following exemplary description liquid scintillator-based Switchillators are used; the techniques described below may also be applied to gases and crystals. In a liquid scintillating medium, fluor molecules (`the solute') can be dissolved in a solvent in order to incorporate them into the liquid. Suitable solvents include, but are not limited to, aromatic organic solvents such as toluene, xylene, dodecyl benzene, diisopropyl naphthalene, phenyl xylyl ethane, and mixtures thereof. The Switchillator fluors can be incorporated into a solid scintillating medium using the same processes that are currently used to incorporate conventional scintillation fluors into a solid scintillating medium.

[0051]   The Switchillator fluors respond to the deposition of energy into the Switchillator by switching from an inactive ("OFF") state to an active ("ON") state. For example, the Switchillator fluors may be activated by ionization from the ground state to a quasi-stable fluorescent state. One process of converting a fluor molecule from an inactive state to an active state is explained as follows. When an ionizing particle, in this case a Compton electron scattered by a gamma-ray, deposits ionizing energy in the solvent of a liquid scintillating medium, excited states are produced in the solvent molecules. These excited states in turn transfer their excitation energy to the fluor molecules, converting them from an OFF state that neither strongly absorbs visible light nor fluoresces, to an ON state that absorbs visible light and fluoresces with high efficiency. The switching of the fluors from their OFF state to their ON state is referred to as activating the fluors. Once activated, the fluors can be excited by the excitation light source of the optical imaging system and the resulting fluorescence can be recorded to produce an image. The activated fluors can be repeatedly excited by the excitation light source in order to extract multiple photons before either reverting to their inactive state, either by a mechanism that is inherent in the material or excitation process, or by being reset using an external mechanism.

PET IMAGING USING SWITCHILLATORS

[0052]   The positions, patterns, and amount of energy deposited by the Compton scatters as a gamma-ray travels on a path through the Switchillator are reconstructed by imaging the fluorescence emitted by the activated fluor molecules. A detailed description of illustrative algorithms and processing steps that can be used to carry out such reconstruction is provided in Example 2. A brief description of steps that can be used to carry out such reconstruction and to use the reconstruction to improve PET imaging of a gamma-ray source are described briefly here.

[0053]   When the optical imaging system is triggered by the FT-photodetector system, the fluorescence detectors (e.g., diode lasers) excite activated fluors and the resulting fluorescence is imaged, repeatedly, by the photodetectors (e.g., CCD cameras). Compton scatters in the Switchillator show up as fluorescing pixels in the image. Clusters of the fluorescing pixels (energy clusters) are identified, wherein each energy cluster is associated with an energy deposition event (Compton scatter) along the path of the gamma-ray in the Switchillator. The pixels in the image can be assigned a statistical weight corresponding to the intensity (brightness) of the background-subtracted fluorescence.

[0054]   A statistical significance can then be assigned to each energy cluster based on the product of the statistical significance values for all of the pixels that make up the energy cluster, such that energy clusters with a greater overall fluorescence intensity are assigned a higher statistical significance. The intensity of the fluorescence is proportional to the number of activated fluor molecules, which is proportional to the deposited ionization energy, with a conversion factor that can be more than 10^4 molecules per MeV. Because the earliest Compton scatters will generally transfer more ionizing energy into the scintillating medium, the energy clusters with a higher statistical significance (i.e., the energy clusters with the highest overall brightness) are more likely to correspond to the earliest Compton scatter and, therefore, an identification of the earliest Compton scatter can be made based on the fluorescence image.

[0055]   Imaging the energy clusters at a higher resolution allows the tracks of the Compton scattered electrons along the trajectory of the gamma-ray to be resolved and recorded based on the location and number of the activated fluor molecules that are imaged. The starting point of the first Compton scattered electron track can be determined on a statistical basis from the evolution of ionization and scattering along the track. In typical solvents the fluor molecules remain within about 10 μm of the point of the energy transfer for many milliseconds, enabling high resolution imaging of the individual Compton electrons from successive Compton scatters in the Switchillator.

[0056]   The information about the locations of the Compton scatters, the energy deposited by the Compton scatters, and the direction of the Compton recoil electrons and scattered gamma-rays, in combination with the constraints placed on the system by Compton kinematics, can be used to recreate the trajectory of the gamma-ray in the Switchillator, to identify the Compton scatter that is most likely to be the earliest Compton scatter, and to identify the starting point of the Compton electron track for the earliest Compton scatter, which corresponds to the location of the first collision of the gamma-ray with an electron. This information can, in turn, be used to identify with high resolution, the end point of an LOR for a coincident gamma-ray pair and to identify and reject false coincidences and other background signals. Background signals from random coincidences, in-patient scatters, and other spurious signal-generating events can be rejected more completely using the full kinematic information of the gamma-ray interactions provided by the PET systems described herein than by the conventional simple energy cut.

[0057]   The many-dimensional parameter space provided by the PET systems described herein lends itself to sophisticated multi-variable analysis methods, including machine learning, event-by-event optimization, and adaptive weighting. Additionally, the methods lend themselves to implementation in real time.

EXAMPLE APPLICATIONS

[0058]   One application of low-dosage, high resolution PET systems described here is the early detection of localized immune response to a pathogen before structural changes, such as early detection of immune system activity in the lungs or extremities of a patient in the case of a respiratory disease such as Covid-19.

[0059]   The system is also useful for total-body screening studies, including those to characterize inflammation or immune response throughout the body. There have been significant reports to develop novel radio tracers for these applications and they would be well matched to the capabilities of the PET systems described here. (Singh, et al., in *The quarterly journal of nuclear medicine and molecular imaging: official publication of the Italian Association of Nuclear Medicine (AIMN) [and] the International Association of Radiopharmacology (IAR), [and] Section of the Society* 54.3 (June 2010), pp. 281-290; and Wu et al., *Theranostics* 3.7 (2013).

[0060]   Another application is the follow-up diagnosis of the serological diagnosis of cancer. An ultra-low dose whole-body scan would provide images for detecting metastasis. Blood tests have been developed which are able to detect signs of cancer in a wide range of organs through identification of mutated DNA or protein biomarkers circulating in the blood. Such assays would be minimally invasive and inexpensive. They could likely detect cancers earlier than any other screening test. However, blood tests provide little or no information about the location of tumors so follow-up imaging would be needed to localize, size, and stage any detected cancer and potential metastases. A recent study showed the value of using conventional PET to follow up on positive results from a blood-based cancer screening assay. (Lennon et al., *Science* 369.6499 (July 2020). The proposed low-cost, total-body, low-dose PET system described here would allow for high-throughput screening of the entire body in any patient with a positive blood test result.

[0061]   Hadron therapy, in which the positron is created by a proton, pion, or neutron, is an application requiring a real-time accurate counting of positron annihilation events at high spatial and energy resolution to monitor the hadron beam and dose.

<u>EXAMPLES</u>

Example 1. Switchillator Design.

[0062]   This example provides illustrative guidance with respect to the selection of Switchillator fluors, using aromatic organic solvent-based scintillating media as examples. The primary considerations in selecting the fluors and designing a Switchillator are achieving high activation yields and low background levels.

Activation Yield:

[0063]   High activation yield for a fluor solute requires efficient energy transfer from the excited states of the solvent to the fluors. When an ionizing particle traverses an aromatic organic solvent the products that survive after 1 ns are mostly low-lying singlet and triplet excited states of the solvent. The singlet states drive conventional scintillation emission by the Förster resonance energy transfer (FRET) mechanism. Both the singlet and triplet states may activate the fluor molecules for subsequent optical excitation. This activation may take the form of converting a non-fluorescent isomer of the fluor (inactive isomer) into a fluorescent isomer (active isomer).

[0064]   By way of illustration, in toluene there are initially 1.35×10^4 singlet excitations per MeV from 10 MeV electrons. (JH Baxendale et al., *Journal of the Chemical Society, Faraday Transactions 1: Physical Chemistry in Condensed Phases* 69 (1973), pp. 771–775.) To achieve a 1% energy resolution at 511 KeV requires 20,000 activated Switchillator fluor molecules per MeV. A process using only singlet excitations of the solvent with an efficiency of 0.4 would provide an energy resolution of $\approx$ 1.5%. In comparison, there are 2.8×10^4 triplet excitations per MeV; a process able to use both triplet and singlet excitations at an efficiency of 0.4 would achieve an energy resolution of 0.8% at 511 KeV deposited.

[0065]   A higher efficiency may be achieved by exploiting alternative mechanisms of activation of the Switchillator fluor. Examples include: 1) the selection of a solvent with enhanced triplet excitations; 2) the use of water-based Switchillators with radical-mediated energy transfer; and 3) radical-mediated energy transfers in other solvents.

[0066]   *Signal-to-Background Ratio.* The fluorescence signal from fluors activated by the gamma-ray is viewed against an intrinsic background signal from fluors activated by the excitation light source. Activation is controlled by: 1) the absorption cross-section of the OFF state of the fluor at the excitation wavelength, $\varepsilon_{OFF}(\lambda_{ex})$; 2) the quantum efficiency of

switching from the OFF state to the ON state, $\Phi_{OFF \to ON}$; 3) the concentration C_{OFF} of inactive (OFF) isomers of the fluor; and 4) the volume V being viewed.

[0067] If the Switchillator is predominately in the OFF state when illumination begins, the appropriate figure of merit is Z_{dye}, the ratio of background resulting from the activation of fluors by the excitation light source to signal from fluors activated by the ionization:

$$Z_{dye} = \frac{\varepsilon_{OFF} \Phi_{OFF \to ON}}{\varepsilon_{ON} \Phi_{ON;fl}} \qquad (1)$$

Z_{dye} is proportional to the ratio of active to inactive fluors in a readout voxel that can be successfully interrogated given some significance threshold. A smaller Z_{dye} allows the use of larger voxels containing more of the uniformly distributed fluors. Conversely, a larger Z_{dye} is permissible if C_{OFF} can be made smaller while maintaining the activation yield by more efficient energy transfer from solvent to solute.

[0068] The Switchillator fluors can be activated by multiple mechanisms, including the excitation light source, previous ionizing gamma-ray interactions, and background ionization. A mechanism for deactivation of activated fluor molecules is consequently usually needed to maintain a stable signal-to-background contrast. Deactivation mechanisms include, but are not limited to, passive deactivation with an appropriate ON state lifetime, active deactivation by optical means, and the inclusion of a deactivating agent. An adequate deactivation lifetime may be achieved by modification of the fluor, the solvent, and/or the Switchillator composition.

[0069] In the case that the only resetting mechanism for the fluor is a reverse isomerization process with quantum efficiency $\Phi_{ON \to OFF}$ from the ON state, continuous illumination by the excitation light source results in a photo-stationary mixture:

$$\frac{C_{ON}}{C_{OFF}} = \frac{\Phi_{OFF \to ON} \varepsilon_{OFF}(\lambda_{ex})}{\Phi_{ON \to OFF} \varepsilon_{ON}(\lambda_{ex})} \qquad (2)$$

[0070] Since each active fluor molecule typically emits $\approx > 50$ photons, for useful Switchillator fluors $\Phi_{ON \to OFF}$ is small, and consequently $\frac{C_{ON}}{C_{OFF}} \gg Z_{dye}$. Fluors which must be deactivated by light have a more demanding requirement on the absorption ratio between active and inactive forms.

[0071] The absorption cross-section at long wavelengths for the OFF state must be sufficiently small to limit activation at the excitation wavelength. The absorption bands of

various fluorescent dyes in solution have a thermal tail at long wavelengths, the Urbach Tail, that falls approximately exponentially

[0072]   The exponential slope coefficient, defined as σ, is called the Urbach steepness coefficient. The absorption cross-section for excitation light of the OFF isomer, $\varepsilon_{OFF}(\lambda_{ex})$, is determined by the product of the slope and the separation of the activation and excitation wavelengths, $\sigma(E_0 - E_{ex})$, where E_{ex} is the energy of the fluorescence excitation light. In the case of multiple exponential tails the cross-section will be dominated by the one with the slowest fall-off.

[0073]   *Illustrative Switchillator Specifications.* The parameters, associated symbols, and desired values for a fluor molecule appropriate for a whole-body PET scanner are presented in Table 1 for the case of energy transfer by singlet excitations of the solvent. The parameter sets and values for different fluors, energy transfer mechanisms, and applications may differ.

[0074]   <u>Table 1</u>: Example properties and values for Switchillator fluor molecules appropriate for a Switchillator-based PET system.

#	Parameter	Symbol	Value	Comment
1	Activation Yield	Y_{act}	$> 5 \times 10^3$	# of ON fluors per MeV deposited
2	Activation Wavelength	Λ_{act}	< 400 nm	Peak OFF to ON wavelength
3	Excitation Wavelength	Λ_{ex}	350-650 nm	At max separation
4	Dye Ratio	Z_{dye}	$< 10^{-10}$	Ratio of background activation rate to fluorescence rate at λ_{ex}, $\dfrac{\varepsilon_{OFF}\Phi_{OFF\rightarrow ON}}{\varepsilon_{ON}\Phi_{ON;fl}}$
5	On-State Lifetime	τ_{ON}	$3 \times 10^{-7} - 10^2$ s	1/e Lifetime of ON fluors in the dark
6	Fluorescence brightness	$\varepsilon_{ON}\Phi_{ON;fl}$	$> 10^3$/(M cm)	Rate of emission from active dye
7	Mean Absorption Length	$\chi(\lambda_{ex})$	> 6 m	1/e absorption length of EL in detector at wavelength λ_{ex}
8	Signal-to-Noise significance	R_s	5σ	Event Significance: product of pixel significances

9	Wavelength of FL	Λ_{fl}	400-700 nm	Wavelength of Fluorescence light
10	# of photons per activated Fluor	N_{fl}	> 50	Mean # of fluorescent photons that can be extracted from an ON fluor before it deactivates

Example 2. Image Acquisition, Processing, and Analysis.

[0075]   This example illustrates methods for acquiring, processing, and analyzing fluorescent images provided by a Switchillator-based PET system. The methods described here are for illustrative purposes only. Other method steps, parameters, and/or algorithms can be used.

[0076]   This example is based on an analysis of a Geant4 simulation of a 511 KeV gamma-ray interacting in a hydrocarbon scintillating medium with H:C equal to 1.96, depicted in FIG. 4. The energy clusters associated with Compton scatters in the Geant4 simulation are shown. The gamma-ray path is indicated with a gray line connecting the locations of Compton scatters. The energy deposition at each scatter is color-coded from blue (low energy fraction) to red (high energy fraction). The gamma-ray loses energy at each Compton scatter until the gamma-ray energy is low enough for the photoelectric effect cross-section to dominate over the Compton process.

Imaging in Pixels

[0077]   Image acquisition begins with the triggering of repeated fluor excitation and imaging cycles by the optical imaging system of an imaging module. After each excitation by the excitation light sources, the fluorescence detector system digitizes the fluorescence from the excited molecules in the Switchillator into a pixelated image.

[0078]   The accurate reconstruction of the earliest gamma-ray interaction point in a Switchillator is facilitated by the pixilation, indexed in the 2D image plane by integers I and j. In the discussion of signal statistical significance below, $N_s(i, j)$ is the number of fluor molecules in pixel (i, j) activated by the deposited energy from a gamma-ray (i.e., signal); $N_b(i, j)$ is the number of fluor molecules activated by the excitation radiation (e.g., laser light) or other mechanisms other than energy deposition by the gamma-ray from an annihilation event (i.e., background).

[0079]   The statistical significance of signal to background in a pixel is given by the ratio of the fluorescence intensity in the pixel to the mean intensity in neighboring pixels that are not involved in the gamma-ray interaction. The statistical significance of signal to background in the pixel, $R_s(i, j)$, in the limit where $N_b \ll N_s$, is given by:

$$R_s(i,j) \equiv \frac{N_s(i,j) + N_b(i,j)}{\sqrt{\langle N_b(i,j) \rangle}}, \qquad (3)$$

where the average number of background molecules per pixel $N_b(i, j)$ can be found as an average of all of the scanned area, or from the illumination of an neighboring quiet area of the detector by the excitation light source.

Identifying Energy Clusters

[0080]   As the Switchillator is scanned, the coordinates of the excitation light beam and the camera frame are recorded with the image. With this 3D information, Compton scattering events can be fully reconstructed, including their location, ionization energy deposition, and the trajectories of the scattered gamma-ray and recoil electron.

[0081]   The gamma-ray interaction will produce a pattern in the fluorescence image corresponding to pixels containing activated fluor molecules that fluoresce with an intensity above background. The pixels can be assigned to energy clusters using image recognition, which can be performed by a variety of pattern recognition or image identification algorithms. An example algorithm implemented in a High Energy Physics 4π-geometry calorimetric detector is presented in Amidei et al., Nucl. Instr. and Meth. A269 (1988), p. 51 and Abe et al., Nucl. Instr. and Meth. A271 (1988), p. 387, and has been applied to Switchillator reconstruction, as described below.

[0082]   The example algorithm starts by identifying `seed' pixels having a high statistical significance (weight) by applying a pre-determined threshold ($T_s$). Pixels with $R_s(i, j)$ above $T_s$ are considered seed pixels. After all seed pixels are found, a lower, `shoulder', threshold T_{sh} is applied to all pixels. Clusters are formed by starting with each seed pixel in turn, adding neighboring pixels that are above T_{sh} and similarly neighbors of neighbors, until completion. Typically, the eight nearest neighbor pixels of a seed pixel are adequate for cluster identification, although the range can be easily expanded. Small gaps can be bridged by applying cluster merging algorithms. The resulting energy cluster is assigned a location, energy, and statistical weight.

[0083] The right-hand panel of FIG. 5 shows a pixelated image of the gamma-ray trajectory of FIG. 4 with a pixel size resolution of 10 mm. The top left panel is an enlarged image of the energy cluster corresponding to the most energetic Compton scatter from FIG. 4 using a pixel size of 10 μm, and the bottom left panel is an enlarged image of the energy cluster corresponding to the second second highest energy Compton scatter from FIG. 4. The density of energy deposition in each pixel is color-coded from blue (low energy fraction) to red (high energy fraction).

[0084] After all energy clusters are found, the statistical significance (weight) for each cluster is given by the product of the statistical significance values of the pixels in the cluster. Thus, the statistical significance, R_s, for each cluster k can be given by:

$$R_s(k) \equiv \prod R_s(i,j) \,,$$

where the multiplication ranges over the pixels in the cluster. A threshold on significance, for example 4σ, is then applied. FIG. 6 shows the result of this algorithm applied to the brightest energy cluster of FIG. 5.

Ordering Energy Clusters by Brightness

[0085] As the number of activated fluors is proportional to the ionization energy, the `brightness' of the pixels in a fluorescence image is related to the energy of the Compton electron. Earlier Compton scatters deplete more of the gamma-ray energy and will, in general, produce brighter pixel clusters with longer electron recoil tracks. This was confirmed by the Geant4 simulations of 511 KeV gamma-rays using the parameters of the liquid scintillator used in the Kamland-Zen detector, a hydrocarbon scintillating medium with H:C equal to 1.96. FIG. 7 shows the number of photons from all Compton scatters (right), and from the most energetic Compton scatter (left).

[0086] FIG. 8 shows a tabulation of the fractional energy in the first five successive Compton scatters. The rows correspond to the fraction of 511 keV deposited in each interaction. The columns represent the interaction number of the gamma-ray, with 1 being the first Compton scatter, tabulated up to the first five scatters. The entries in the table are event counts out of 10,000 simulated gamma-rays. The brightest event cluster is produced by the earliest Compton scatter approximately 55% of the time, the second Compton scatter 25% of the time, and the third Compton scatter 11% of the time.

Constructing a Line-of-Response

[0087] The LOR is the line drawn between the initial gamma-ray interaction points in the Switchillators of two imaging modules. FIG. 11 shows an example LOR drawn between the first Compton scattering event in each of two opposing imaging modules, in the case of no scattering in the patient. A LOR reference system is defined here as the orthogonal directions along (longitudinal) and transverse to the LOR. The optical imaging system provides improved spatial resolution of the LOR for a positron-electron annihilation event by identifying, on a statistical basis, the location of the earliest energy-deposition event for each gamma-ray of a coincident pair. FIG. 9 shows the longitudinal [Left] and transverse [Right] positions of the brightest interaction between the 511 keV gamma-ray and the scintillating medium in the line-of-response reference frame in the Kamland-Zen hydrocarbon scintillating medium.

[0088] The pixelated images of the energy clusters provide information on the direction of the Compton recoil electron after a Compton scattering event, which can be used to identify the end points of a LOR. Because the scattering angle of a Compton scattered gamma-ray and its recoil electron are completely constrained by 2-body Compton kinematics (Compton, *Phys. Rev.* 21 (5) (1923), pp. 483-502), the geometric pattern of energy clusters in the pixelated optical image enables a fit to the locations, brightness (energy deposition), and/ recoil directions from which the path and entry point of a gamma-ray in the scintillating medium can be reconstructed. Moreover, once the energy cluster corresponding to the first gamma interaction has been identified, the starting end of the Compton-scattered electron track, which corresponds to the first gamma-ray/electron collision point can be determined, on a statistical basis, based on energy loss and scattering along the imaged electron track, and by the Compton 2-body kinematic constraints on the energies and spatial relationships among clusters.

[0089] FIG. 10 shows a table of annihilation event counts partitioned by whether the first energy deposition for one, both, or neither gamma-ray for a coincident gamma-ray pair was the most energetic Compton scatter in the module, and further partitioned by whether the starting point of the recoil electron track for one, both, or neither of the gamma-rays was correctly reconstructed. For the Compton scatters where the starting end of the electron track was correctly identified, the impact parameter of the LOR for the coincident gamma-ray pair compared to the true annihilation point is plotted. In the case where both of the first interactions are the most energetic Compton scatters, the impact parameter is almost always less than 30 μm, when the voxel size is 20 μm. For events in which both gamma-ray

interactions are correctly reconstructed, the resolution on the LOR is characterized by the voxel size, typically 10-30 μm. If either first interaction is not the most energetic Compton scatter, the median impact parameter is 35 millimeters and the contrast is low.

[0090] The precision of the LOR can be further improved based on iterative imaging of the fluors, with the possibility of hundreds to many thousands of excitations for the same activated fluor pattern. The example optical system of FIGS. 2 and 3 is designed to enable advanced imaging that supports a number of techniques, including successively increasing magnification, optical steering of the exciting light and the camera imaging paths, multiple wave-length excitations, time-dependence of the fluorescence allowing for the use of multiple fluors, and optimization of specific sub-measurements.

[0091] The ability to perform iterative imaging is ideal for real-time adaptive imaging, in which the imaging algorithm parameters are optimized on the accumulated image at each time, and on machine learning. The parameters include kinematic information from each scattering event, relative ordering and brightness of the scatters and prior information from the accumulating sample image.

[0092] FIGS. 12 and 13 illustrate how the optical imaging system can used to further improve the reconstruction of a gamma-ray source by identifying and eliminating false coincidences. FIG. 12 shows an example LOR drawn between the first Compton scatter in each of two opposing imaging modules in the case where one gamma-ray has undergone in-patient scattering. LORs that are mis-measured due to gamma-ray in-patient scattering will typically be distributed over an area large compared to the feature resolution, and can be background-subtracted.

[0093] The two-body kinematics of Compton scattering allows an additional rejection of annihilation events with in-patient scattering. As shown in FIG. 13, the recoil electron and the Compton scattered gamma-ray momenta define a plane in which the LOR for a coincident gamma-ray pair must lie. The statistical significance of the deviation from this plane can be used as a factor in the event weight during gamma-ray source image reconstruction.

Spatial Resolution along a Line-of-Response

[0094] The Switchillator-based PET systems accommodate advanced Time-of-Flight (TOF) techniques for identifying an annihilation event with high spatial resolution along a LOR. In addition, the connection between the Switchillator and TOF systems goes both directions: the TOF system provides seeds locations for the Switchillator spatial cluster

finding, and then, after full analysis of the gamma-ray trajectories in the modules, the Switchillator system uses the precise spatial information to sharpen the TOF results. Sharpening the probability distribution of the vertex position along the LOR both provides a more significant image and diminishes background events from fluor molecules excited by sources other than the scattered electron.

[0095]   The spatial resolution along the LOR is determined by the location of the interactions of each gamma-ray in its respective module, the response time and yield of the scintillating medium, the details of collecting the scintillation light in the module, and the relative timing of the arrival of the two gamma-rays. A simulation of 1000 gamma-ray interactions in the Kamland-Zen scintillator finds >2000 scintillation photons are produced in the wavelength range 360-785 nm.

[0096]   FIG. 14 shows the transit time between the gamma-ray entry at the front face (t=0) and the first photon to arrive at the FT-photodetector for direct and reflected photons in the example implementation of FIGS. 2 and 3. FIG. 15 shows the distribution of FIG. 14 corrected for the photon transit time, assuming the photons were emitted from the brightest cluster.

[0097]   FIG. 16 shows the intrinsic TOF resolution distribution for annihilations in the sample from a Geant4 simulation with an infinitely fast scintillator. The TOF resolution may be determined y by the speed and yield of the scintillator fluor (Drew R. Onken et al. *Mater. Adv.* 1 (1 2020), pp. 71–76. doi: 10.1039/D0MA00055H. url: http://dx.doi.org/10.1039/D0MA00055H.), as the LAPPD detector in the example implementation has single photon resolution less than 50 psec.

[0098]   In addition to scintillation light, there is a small production of Cherenkov light, weighted toward the early Compton scatters for which the gamma-ray has a higher energy and so a higher probability of producing an electron with velocity over Cherenkov threshold. Selecting the earliest photon enhances these photons. In addition, the LAPPD records the position of detected Cherenkov photons for comparison with prediction.

Ultra-Low-Dose High-Resolution PET Imaging

[0099]   The high spatial resolution for individual positron-electron annihilations allows the formation of useful PET images with significantly lower radiation dose to a patient than in current practice.

[00100]   FIG. 17 presents the specifications (center) and figures (left and right) of the commercially available Standard Jaszczak Phantom™ (Biodex Medical Systems, Inc, *"Nuclear Medicine and molecular imaging, devices and supplies"*; Catalog 125, pg. 84, Model No. 043-762, 2020) used to test and calibrate PET and SPECT scanners. The phantom contains cylinders filled with a radioactive tracer solution (`hot rods'), in a tight-fitting volume filled with a solution containing a lower tracer concentration (background).

[00101]   The left-hand panel of FIG.18 shows the simulated annihilation coordinates for the Jaszczak phantom described in FIG. 17. The center panel displays the filtered back-projection (Dudgeon and Mersereau, *"Multidimensional digital signal processing"*. Prentice-Hall, 1984) of the left panel, with a pixel size of 1 mm. The right-hand panel displays the center panel smoothed by a gaussian filter of 2 mm. The hot rods are loaded with 300 Bq/ml of ^{18}F, while the background is loaded with 100 Bq/ml of ^{18}F, concentrations that are a factor of 100 lower than typical practice in human patients. The efficiency of reconstructing the LOR to within a sigma of 20 μm is assumed to be 10%; the scanner is assumed to have a radius of 30 cm and an axial length of 18 cm; and the exposure time is 10 minutes. It should be noted that the line-integral of background in this simulated geometry is smaller than would be encountered in a patient.

[00102]   The left-hand panel of FIG. 19 shows the simulated annihilation coordinates for the Jaszczak phantom described in FIG. 18, but with two additional cylinders of 10 mm length and the same diameter, but without hot rods, added to each end in order to simulate additional background from a longer line-integral. The center-panel displays the filtered back-projection of the left-hand panel, with a pixel size of 1 mm. The right-hand panel shows the center panel smoothed by a gaussian filter of 2 mm. As in the case of FIG. 18, the hot rods are loaded with 300 Bq/ml of ^{18}F, while the background is loaded with 100 Bq/ml of ^{18}F, concentrations that are a factor of 100 lower than typical practice in human patients. The efficiency of reconstructing the LOR to within a sigma of 20 μm is assumed to be 10%; the scanner is assumed to have a radius of 30 cm and an axial length of 18 cm; and the exposure time is 10 minutes.

[00103]   The word "illustrative" is used herein to mean serving as an example, instance, or illustration. Any aspect or design described herein as "illustrative" is not necessarily to be construed as preferred or advantageous over other aspects or designs. Further, for the purposes of this disclosure and unless otherwise specified, "a" or "an" means "one or more."

[00104] The foregoing description of illustrative embodiments of the invention has been presented for purposes of illustration and of description. It is not intended to be exhaustive or to limit the invention to the precise form disclosed, and modifications and variations are possible in light of the above teachings or may be acquired from practice of the invention. The embodiments were chosen and described in order to explain the principles of the invention and as practical applications of the invention to enable one skilled in the art to utilize the invention in various embodiments and with various modifications as suited to the particular use contemplated. It is intended that the scope of the invention be defined by the claims appended hereto and their equivalents.

WHAT IS CLAIMED IS:

1.   A PET system comprising a plurality of imaging modules, the imaging modules comprising:

a scintillator compartment containing a scintillating medium comprising one or more fluors, the scintillator compartment having a front face and a transparent back face;

a photodetector system comprising one or more photodetectors optically coupled to the scintillator compartment and configured to detect scintillation photons generated in the scintillating medium;

an optical imaging system comprising:

      one or more excitation light sources optically coupled to the scintillator compartment and configured to direct excitation light onto the scintillating medium; and

      one or more fluorescence detectors optically coupled to the scintillator compartment and configured to detect fluorescence generated by the fluors in the scintillating medium.

2.   The PET system of claim 1, wherein the scintillation medium is a liquid medium.

3.   The PET system of claim 1 or claim 2, wherein the one or more photodetectors comprise one or more diode lasers.

4.   The PET system of any of claims 1-3, wherein the one or more fluorescence detectors comprise one or more CCD cameras.

5.   The PET system of any of claims 1-4, wherein the photodetector system is a TOF photodetector system.

6.   The PET system of any of claims 1-5, wherein the one or more photodetectors are optically coupled to a transparent back surface of the scintillator compartment and an opposing internal front surface of the scintillator compartment is reflective.

7.   The PET system of any of claims 1-6, wherein the scintillating medium comprising one or more fluors is contained within a first sub-volume adjacent to a front

surface of the scintillator compartment and the scintillator compartment further comprising a second sub-volume of scintillating medium that is free of the one or more fluors, but is optically matched with the scintillating medium comprising one or more fluors.

8.   A method for imaging a sample using the PET system of any preceding claim, the method comprising:

positioning a sample within an imaging volume defined by the plurality of imaging modules, wherein positron-electron annihilation events in the sample generate coincident gamma-ray pairs;

detecting scintillation photons generated by the interaction of each gamma-ray of a coincident gamma-ray pair with the scintillating media in two opposing imaging modules using the photodetectors to identify an initial lines-of-response for the coincident gamma-ray pair;

triggering the excitation light sources to excite fluors in the scintillating medium of each imaging module;

recording fluorescence emitted by the excited fluors to generate an image of energy clusters corresponding to Compton scatters of the gamma-rays in the scintillation material;

identifying the energy cluster corresponding to the earliest Compton scatter for both of the gamma-rays;

determining the energy, trajectory and direction of the Compton scattered electrons for the earliest Compton scatters to identify the location of a first collision between the gamma-ray and an electron in the scintillating medium for both of the gamma-rays; and

improving the resolution the line-of-response for the coincident gamma-ray pair, by using the locations of the first collisions as end points for the line-of-response.

9.   The method of claim 8, further comprising improving the resolution the line-of-response for the coincident gamma-ray pair using the totality of information on the reconstructed plurality of spatial and temporal images on the successive Compton scatters of the two gamma-rays.

APPENDIX – Various Additional Embodiments of the TOF-PET Systems

[00105]   (IONIZATION-ACTIVATED TWO-STATE ORGANIC FLUORS for TOF-PET: SWITCHILLATORS)

1. The use of ionization-activated fluors as a component of the scintillator medium in a PET or TOF-PET detector

2. Embodiment 1 in which the ionization-activated fluors include two-state organic fluors ('Switchillator') as a component of the scintillator medium in a PET or TOF-PET detector;

3. Embodiment 2 in which the Switchillator is activated to a fluorescent-capable state (ON state) by ionization energy deposited by a gamma-ray, X-ray, or photon of other energy.

4. Embodiment 2 in which the Switchillator is activated to a fluorescent-capable state (ON state) by ionization energy deposited by a charged particle;

5. Embodiment 2 in which the Switchillator is activated to a fluorescent-capable state (ON state) by ionization energy deposited by charged particles produced in interactions in the scintillator medium;

6. Embodiment 2 in which the Switchillator in the ON state can be repeatedly excited to the fluorescent state;

7. Embodiment 2 in which there exists a mechanism for the Switchillator to de-activate from the ON state to the non-fluorescent-capable (OFF) state;

8. Embodiment 2 in which the scintillator medium is a liquid;

9. Embodiment 2 in which the scintillator medium is a solid;

10. Embodiment 2 in which the scintillator medium is a gas.

[00106]   (DETECTOR SYSTEM)

11. An imaging time-of-flight positron-emission tomography detector system based on Embodiment 2 comprising:

(a) a sample volume in which the patient, animal, material, or other sample can be installed;

(b) modules containing liquid scintillator material, each module having a front face, a back face, and four side faces, with the front face contiguous to the sample volume;

(c) the liquid scintillator or some sub-volume thereof to serve as a solvent for ionization-activated organic fluor molecules;

(d) each module typically to have a corresponding module symmetrically-placed diametrically on the other side of the sample volume;

(e) each module instrumented with a time-of-flight optical system that includes at least one photodetector with high spatial and temporal resolution on one or more module faces viewing the liquid;

(f) the time-of-flight optical system may additionally include a mirror or system of mirrors on one or more module faces viewing the liquid;

(g) the time-of-flight optical system may include light-absorbing mechanisms on one or more module faces or in the volume;

(h) each module instrumented with a time-of-flight electronics system to determine the time of the gamma-ray interaction in the module;

(i) each module instrumented with at least one source of photons such as, but not limited to, a laser diode to excite the fluor molecules at specified wave-lengths after fluor activation by ionization;

(j) each module instrumented with an optical system capable of focusing and steering the beam or beams of exciting photons;

(k) each module with an optical transition region between any optical devices and an active volume containing the compound of Embodiment 2, the transition region serving as an optical lever arm;

(l) each module instrumented with an optical camera system capable of a 3-dimensional reconstruction of the position and topology of the gamma-ray interaction in the liquid;

(m) each module instrumented with an optical system capable of focusing and

steering the camera system;

(n) each module instrumented with data acquisition and processing systems for real-time analysis and image optimization

[00107]   (TIME-OF-FLIGHT SYSTEM)

12. The detector system of Embodiment 11 comprising:

(a) The detector system of Embodiment 11, wherein the photodetectors are configured to accommodate the operation of the optical camera system and photon source.

(b) The detector system of Embodiment 11, wherein the photodetector system includes a mirror or mirrors.

(c) The detector system of Embodiment 11, wherein the photodetectors have spatial resolutions of 3 mm (sigma) or better for a single photon.

(d) The detector system of Embodiment 11, wherein the photodetectors have spatial resolutions of 1 mm (sigma) or better for a single photon.

(e) The detector system of Embodiment 11, wherein the photodetectors have time resolutions of 50 psec (sigma) or better for a single photon.

(f) The detector system of Embodiment 11, wherein the photodetectors have time resolutions of 25 psec (sigma) or better for a single photon.

(g) The detector system of Embodiment 11, wherein the photodetectors are fast multi-channel vacuum photomultipliers such as but not limited to, LAPPDs.

(h) The detector system of Embodiment 11, wherein the photodetectors are solid-state photodetectors such as, but not limited to, SiPMs.

(i) The time-of-flight system of Embodiment 12 in which the time of the gamma-ray interaction in the scintillator is determined by time and position of the earliest detected photon.

(j) The time-of-flight system of Embodiment 12 in which the time of the gamma-ray interaction in the scintillator is determined by the times and positions of the several earliest detected photons.

(k) The time-of-flight system of Embodiment 12 in which the time of the gamma-ray

31

interaction in the scintillator is refined by processing of the times and positions of the several earliest detected photons and an analysis of the light yield, topology and kinematics of the reconstructed gamma-ray Compton scatterings.

(l) The method of Embodiment 12 in which the light yield of the several identified Compton scatterings is used to weight the time-ordering of the scatterings.

[00108]   (IMAGING SYSTEM)

13. The detector system of Embodiment 11 wherein the optical camera system consists of one or more cameras viewing the module in a stereo configuration.

14. The detector system of Embodiment 11 wherein the optical cameras are digital with electronic readout.

15. The detector system of Embodiment 11 wherein the optical cameras are capable of resolving 25μm by 25μm pixels in the sample volume.

16. The detector system of Embodiment 11 wherein the optical cameras are capable of resolving 10μm by 10μm pixels in the sample volume.

17. The detector system of Embodiment 11 wherein the source of exciting photons consists of one or more controllable independent units;

18. The detector system of Embodiment 11 wherein the exciting source can be steered by the optics system over the scintillator module active volume.

19. The detector system of Embodiment 11 wherein the exciting source can be optically focused over the scintillator module active volume.

20. The detector system of Embodiment 11 wherein the exciting source can be optically focused independently in the horizontal and vertical planes.

21. The detector system of Embodiment 11 wherein the exciting source can be optically focused independently to 100μm in the horizontal and vertical planes.

22. The detector system of Embodiment 11 with associated computational hardware and soft- ware to control, sequence, and record the process steps in imaging the gamma-ray interactions in the module;

23. The detector system of Embodiment 11 with associated computational hardware and software to control and record the analysis of the images of the individual gamma-ray Compton scatters in the module to statistically determine the location of the first interaction of the gamma-ray in the fluor.

24. The detector system of Embodiment 11 with associated computational hardware and software to control and record the analysis of the images of the individual gamma-ray Compton scatters in the module to statistically determine the location of the second interaction of the gamma-ray in the fluor.

25. The detector system of Embodiment 11 with associated computational hardware and software to control and record the analysis of the images of the individual gamma-ray Compton scatters in the module to statistically determine the location of a plurality of the interactions of the gamma-ray in the fluor.

26. The detector system of Embodiment 11 with associated computational hardware and software to control and record the analysis of the images of the individual gamma-ray Compton scatters in the module to statistically determine the trajectories, including the interaction gamma-electron scattering point, of the electrons arising from interactions of the gamma-ray in the fluor.

27. The detector system of Embodiment 11 with associated computational hardware and software to control and record the analysis of the images of the individual gamma-ray Compton scatters in the module to statistically determine the trajectory of the gamma-ray from the energies, separations, and relative angles of the electrons arising from interactions of the gamma-ray in the fluor.

28. The detector system of Embodiment 11 with associated computational hardware and software to select coincidences in time between interactions in multiple modules.

29. The detector system of Embodiment 11 with associated computational hardware and software to coordinate the control, sequence, and record the process steps in imaging the gamma- ray interactions in multiple modules;

30. The detector system of Embodiment 11 with associated computational hardware and soft-ware to calculate in real-time the line-of-response between the locations of the first interactions of gamma-rays recorded in two modules;

31. The detector system of Embodiment 11 with associated computational hardware and software to calculate in real-time the position of the positron-electron annihilation from the line-of-response and the TOF system results in the first and second liquid scintillator modules.

32. The detector system of Embodiment 11 with associated computational hardware and software to control and record the analysis of the images of the individual gamma-ray Compton scatters in the module to statistically reject in-patient scattering using the energies, separations, and relative angles of the electrons arising from interactions of the two gamma-rays in the fluor.

[00109]   (SOLVENT and FLUOR)

33. The detector system of Embodiment 11, wherein an organic fluor is a component of the liquid scintillator material;

34. The detector system of Embodiment 30, wherein the liquid scintillator materials are organic solvents.

35. The detector system of Embodiment 30, wherein the liquid scintillator materials are water- based scintillator materials.

36. The detector system of Embodiment 30, wherein the fluor has both at least one non-fluorescent state and at least one fluorescent state.

37. The detector system of Embodiment 30, wherein the fluor can be switched from a non-fluorescent state to a fluorescent state.

38. The detector system of Embodiment 30, wherein the fluor is a fluorescent dye that can be activated from a non-fluorescent state to a state capable of excitation to fluorescence by ionization energy deposited by an incident charged particle or gamma radiation.

39. The detector system of Embodiment 30, wherein the fluor is a fluorescent dye that can be de- activated from a state capable of excitation to fluorescence to a non-fluorescent state by photon excitation, chemical reaction, or a physical process.

40. The detector system of Embodiment 34, wherein the fluor can be excited by light to a state that fluoresces.

41. The detector system of Embodiment 34, wherein the fluor can be excited by light to a state that fluoresces and returns to the activated state.

42. The detector system of Embodiment 34, wherein the fluor can be repeatedly excited by light to a state that fluoresces and returns to the activated state.

43. The detector system of Embodiment 35, wherein the ratio of the activation of the fluor in the deactivated state to the excitation in the activated state is less than 10^{-10} at room temperature.

44. The detector system of Embodiment 35, wherein the ratio of the activation of the fluor in the deactivated state to the excitation in the activated state is less than 10^{-15} at 0 °C.

[00110]   (IMAGE RECONSTRUCTION)

45. The detector system of Embodiment 30 with the capability in each module of a coincident pair to:
   - identify a plurality of Compton scattering energy deposition events resulting from an interaction of a gamma-ray from a coincident gamma-ray pair in the liquid scintillator/fluor volume;
   - measure the locations of the individual optical-photon-emitting Compton-scattering events at a resolution of 50 microns or less;
   - measure the locations of the individual optical-photon-emitting Compton-scattering events at a resolution of 10 microns or less;
   - measure the locations of the individual optical-photon-emitting Compton-scattering events at a resolution of 2 microns or less;
   - measure the recoil electron energy in each Compton-scattering from the number and spatial distribution of fluor molecules activated by ionization ('brightness') in the individual Compton-scattering events;
   - measure the direction of the recoil electron in each Compton-scattering;

- assign weights to the individual clusters most likely to be the initial scatter of the gamma-ray from the annihilation. from the full information of the relative measured positions, angles, brightness and electron recoil direction.

- From the kinematics of the scattering and the measurements of the recoil electron, determine the initial direction of the gamma-ray in the series of Compton Scattering events in the module.

46. The detector system of Embodiment 30 with the capability of correlating the measurements in the modules of a coincident pair to:

- calculate the line-of-response (LOR) between the calculated initial gamma-ray Compton scatter in each module;

- refine the LOR using the correlated angular and energy information in the two modules;

- calculate the probability of scattering in the patient for each of the gamma-rays;

- calculate the annihilation source position in the sample volume using the combined LOR and time-of-flight information;

- calculate a weight for the event;

- generate an image of a gamma-ray-emitting region in the sample based on the calculated source positions and weights from multiple annihilation events.

- re-optimize the image and enhance contrast by correlating the detailed angular, spatial, and energy information in the event with the cumulative image.

[00111]   (ENERGY RESOLUTION)

47. The method of Embodiment 41, wherein the energy of each gamma-ray is determined from fluorescent light from the excitation of activated molecules.

48. The method of Embodiment 41, wherein the energy of each gamma-ray is determined from parameters of the interactions of each of the gamma-rays.

49. The method of Embodiment 41, wherein the energy of each gamma-ray is determined from the entirety of the information.

50. The method of Embodiment 41 employing machine learning and algorithms of artificial intelligence to tune the energy calibrations for each module as the exposure evolves.

[00112]   (SOURCE SPATIAL RESOLUTION)

51. The method of Embodiment 41, wherein the position of the source of the two photons is determined from the line of response between the reconstructed interaction points of the two gamma-rays.

52. The method of Embodiment 41, wherein the position of the source of the two photons is determined from the entirety of the information on the two gamma-rays, including but not limited to the reconstructed interaction points, directional information on the gamma-ray showers, and the reconstructed energies.

53. The method of Embodiment 41, wherein the position of the source of the two photons is determined from the entirety of the information on the two gamma-rays, including but not limited to the reconstructed interaction points, directional information on the gamma-ray-induced showers, and the reconstructed energies and the prior information contained in the evolving reconstructed image.

54. The method of Embodiment 49 employing machine learning and algorithms of artificial intelligence to maximize signal-to-noise for each event as the reconstructed image evolves.

55. The method of Embodiment 49 employing machine learning and algorithms of artificial intelligence to maximize the number of events included in the analysis, including events in which one or both gamma-rays have significant energy losses due to scattering or absorption.

[00113]   (APPLICATIONS)

56. The method of Embodiment 41, wherein the position of the source of the two photons is determined.

57. The method of Embodiment 30, wherein the sample is a human patient.

58. The method of Embodiment 30, wherein the sample is an animal.

59. The method of Embodiment 30, wherein the sample is an organic or inorganic material.

60. The method of Embodiment 30, wherein the source of the emitted gamma-ray pairs in the sample is a positron-emitting radioisotope.

61. Embodiment 1 delivering a 'Ultra-Low^{TM}' radioactive dose to a patient of at least 50 fold less than the typical dose of 5-10 mSv for early detection of immune or inflammatory response to virus or disease.

62. Embodiment 57 in which the dose reduction is enabled by one or more of: longer exposures, lower required resolution including relaxing cuts on in-patient scattering, sensitivity to the whole body without scanning, and targeted signatures of inflammation.

63. Embodiment 1 for PET or TOF-PET imaging as follow-up to serological detection of cancer or other disease.

64. The method of Embodiment 30, wherein the source of the emitted gamma-rays is the plurality of annihilations of positrons from a beam of hadrons directed into the sample.

65. Embodiment 57 in which the dose reduction is enabled by one or more of: longer exposures, lower required resolution including relaxing cuts on in-patient scattering, sensitivity to the whole body without scanning, and targeted signatures of inflammation or immune response.

66. Embodiment 1 for PET or TOF-PET imaging as follow-up to blood-based detection of cancer or other disease.

67. Embodiment 59 in which the purpose of the PET or TOF-PET is to localize the primary tumor.

68. Embodiment 59 in which the purpose of the PET or TOF-PET is to detect and localize metastases of the primary tumor.

69. Embodiment 59 in which the purpose of the PET or TOF-PET is to stage the cancer.
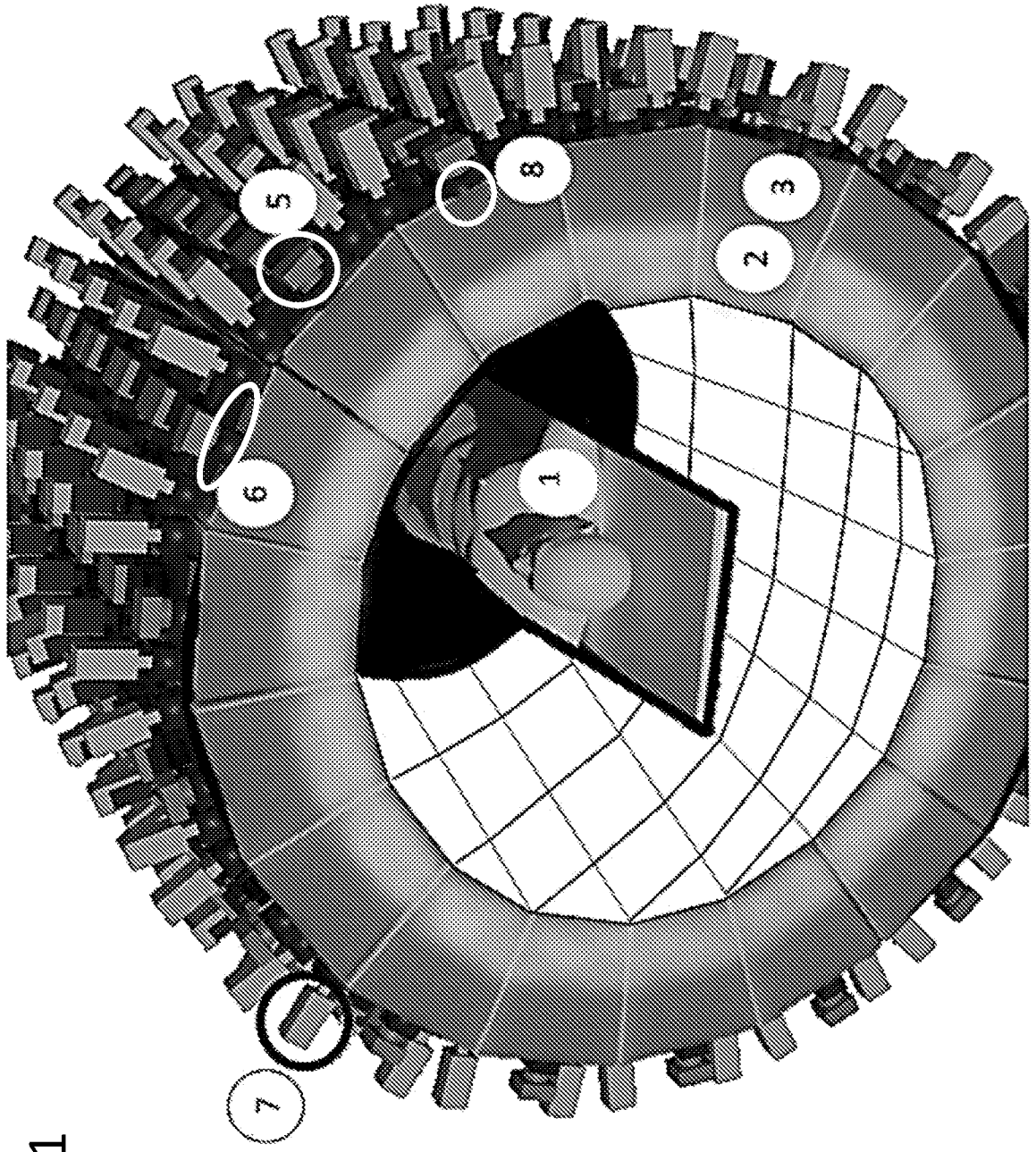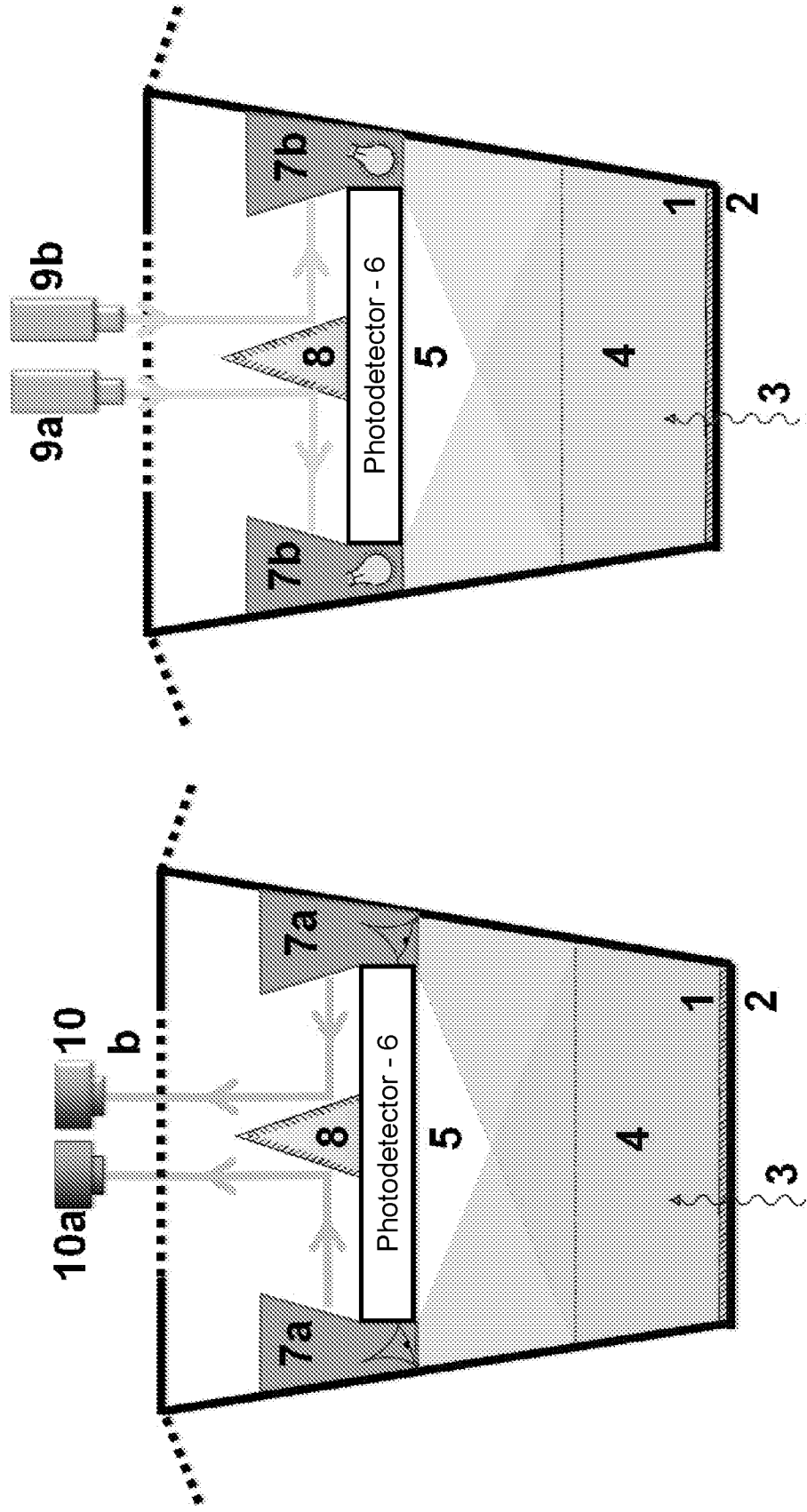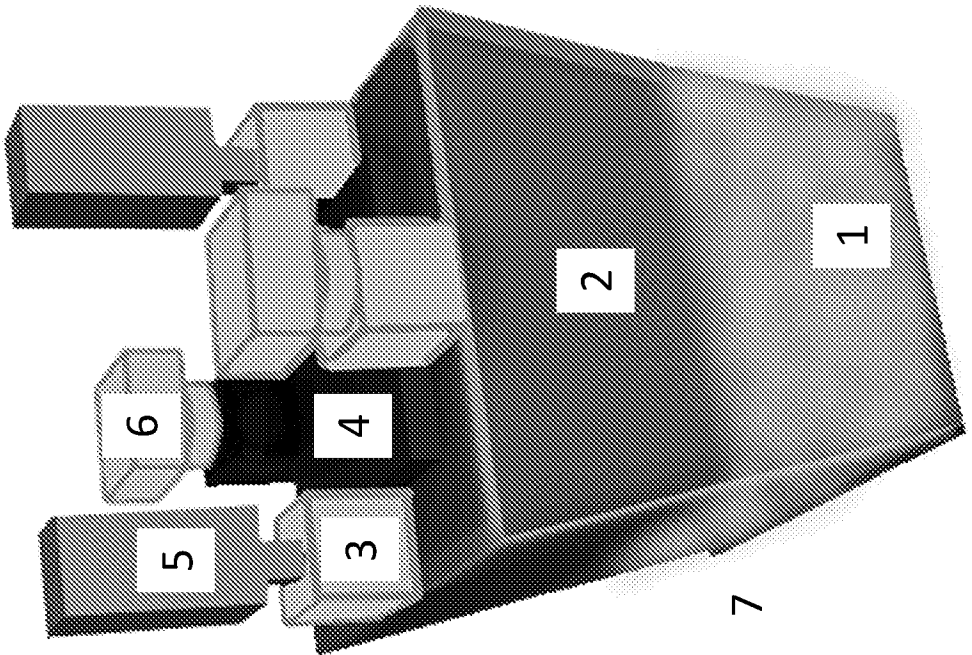
FIG. 1

FIG. 2
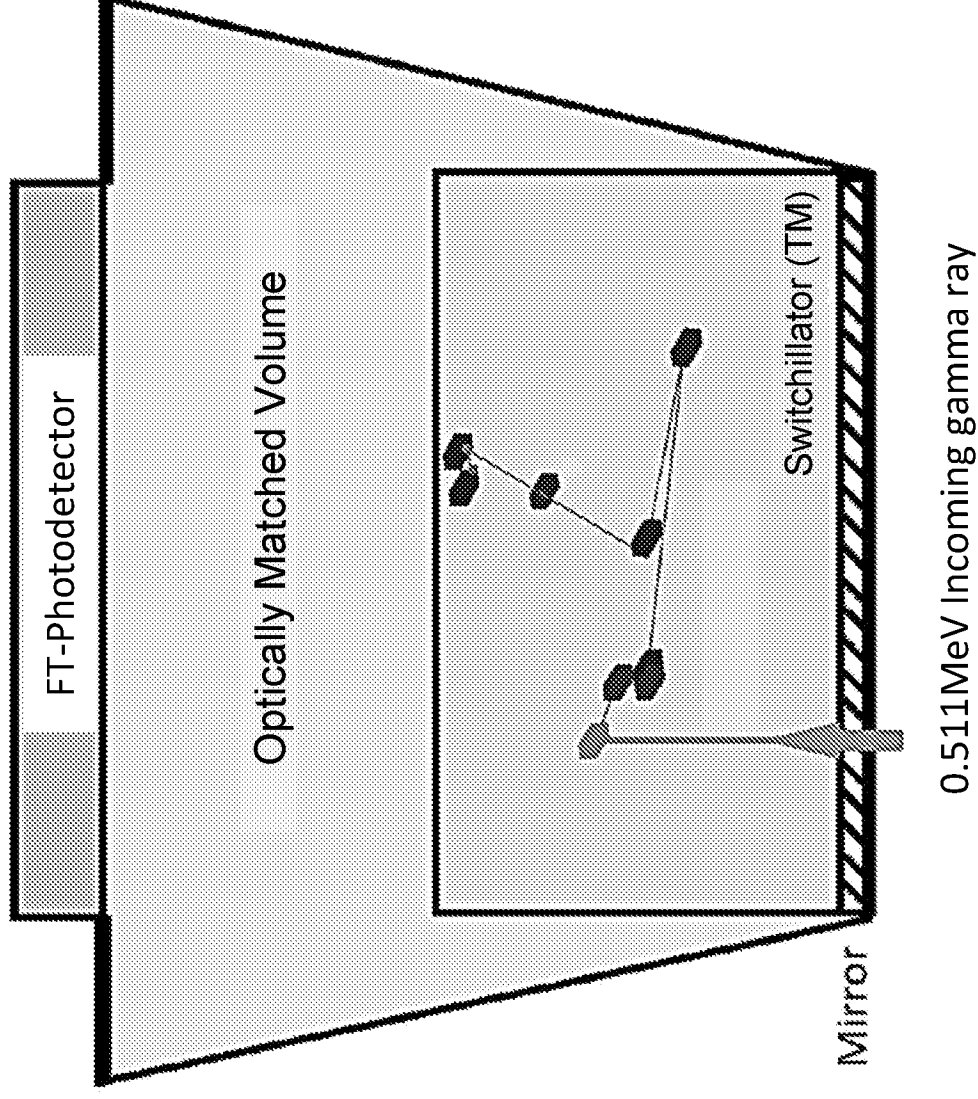
FIG. 3

FIG. 4

FT-Photodetector

Optically Matched Volume

Switchillator (TM)

Mirror

0.511MeV Incoming gamma ray

FIG. 5

Gamma path and registered photon creation clusters.
Red indicates more photons, units of 10 mm

3d Brightest cluster, in units of 10 microns
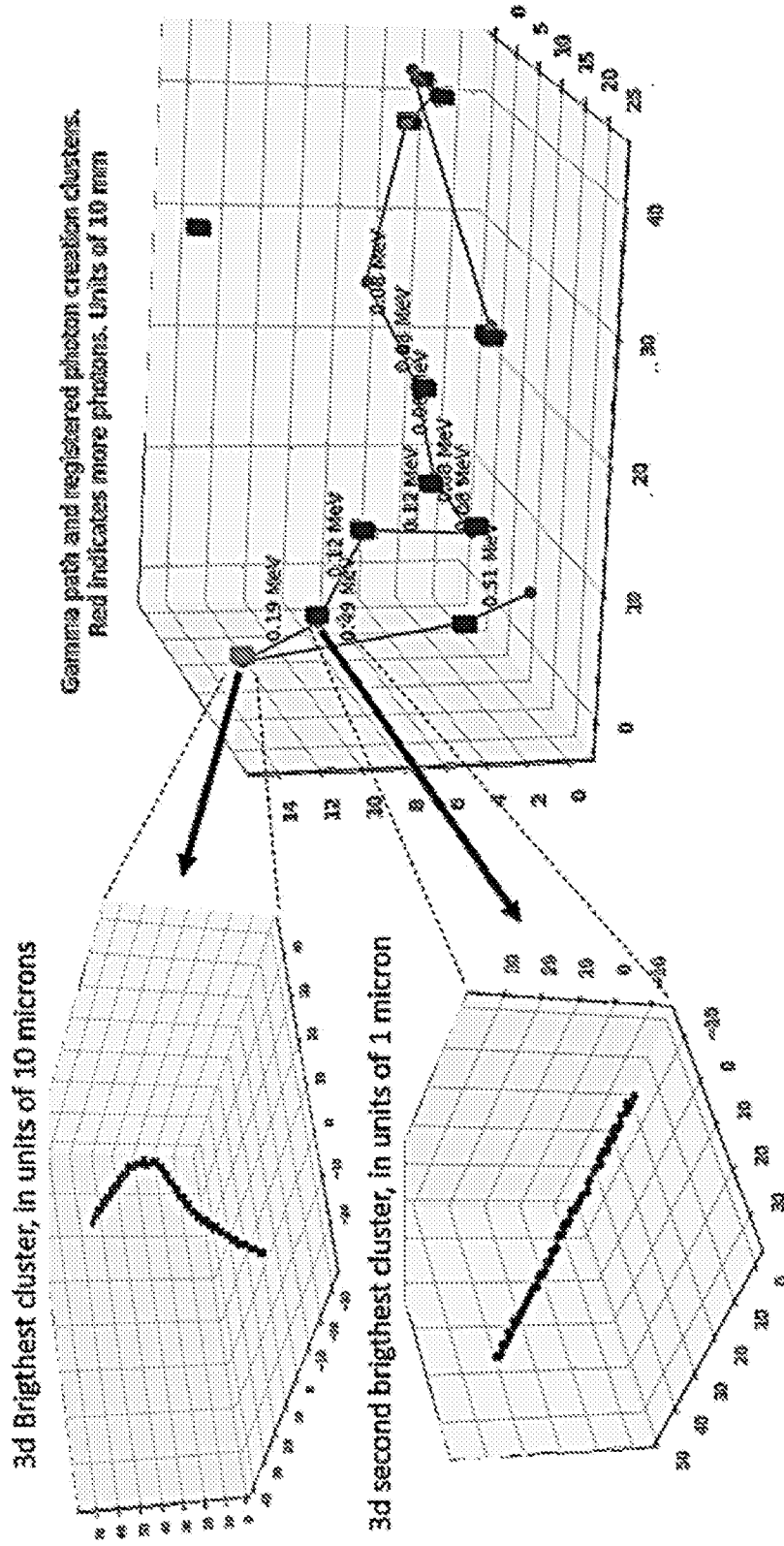
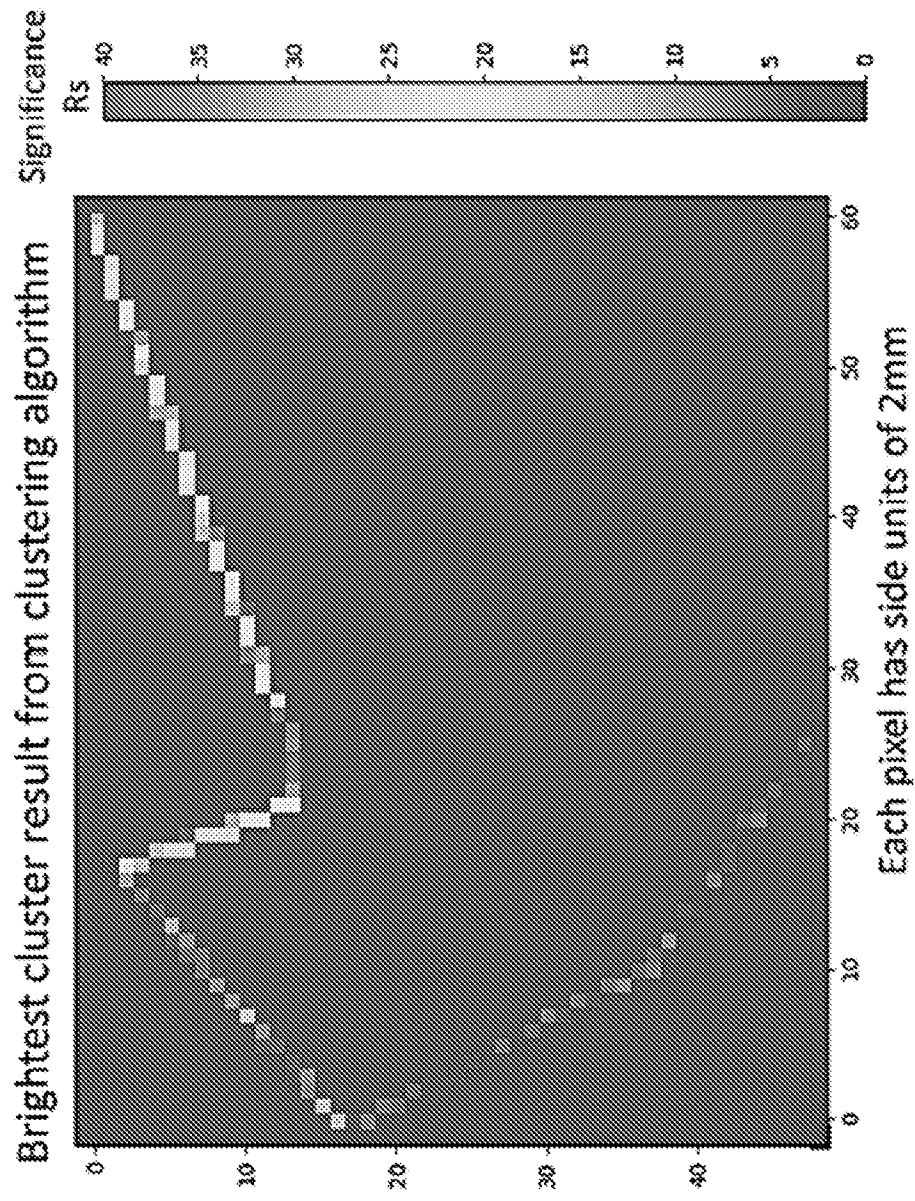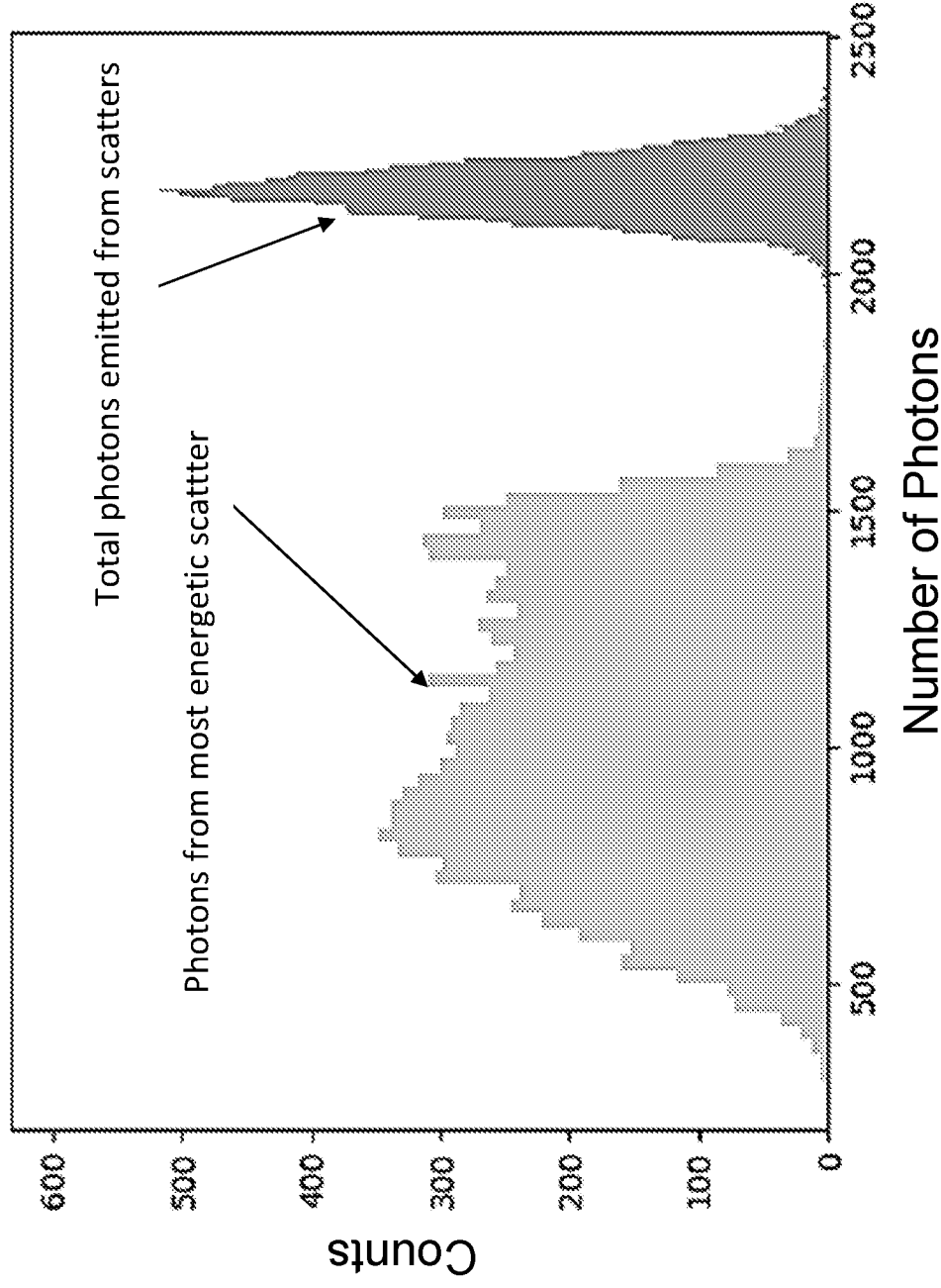3d second brightest cluster, in units of 1 micron

FIG. 6

Section: 511 Gamma Energy Deposition

FIG. 7

Scintillation photons from the most energetic Compton scatter and from the entire sequence of scatters in a liquid scintillator by a 511keV gamma, 10000 events.

Section: 511 Gamma Energy Deposition

FIG. 8

Differential Energy deposited at interaction, 10000 events

Differential Energy deposited, percentage of 511keV

	1	2	3	4	5
70	1568	101	5		
60	1532	450	66	3	
50	1306	710	229	56	3
40	1212	1049	514	115	40
30	1320	1505	959	452	150
20	1463	2618	2555	1747	1002
10	1596	3552	5642	7560	8685

Interaction Number
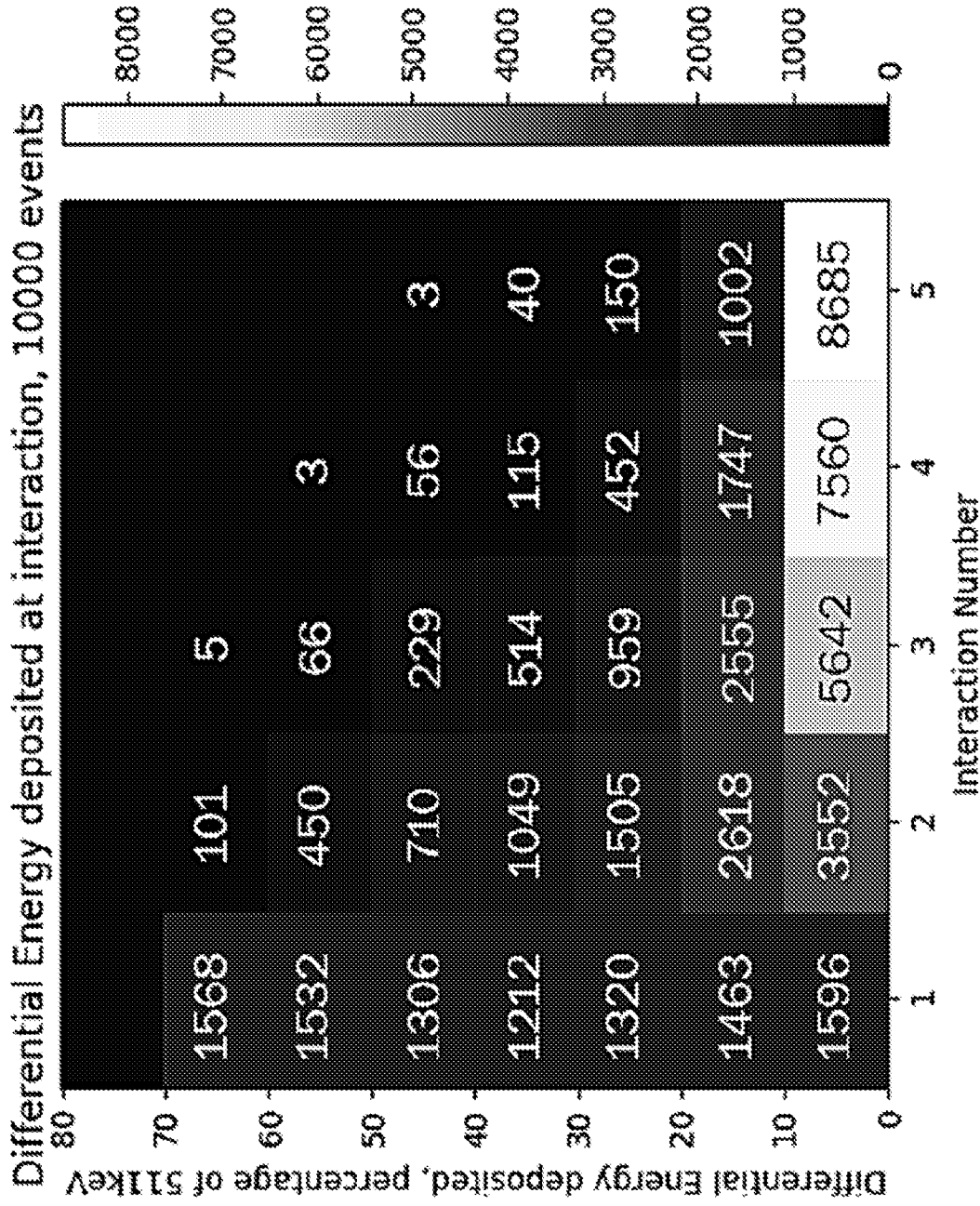
Section: 511 Gamma Energy Deposition

FIG. 9

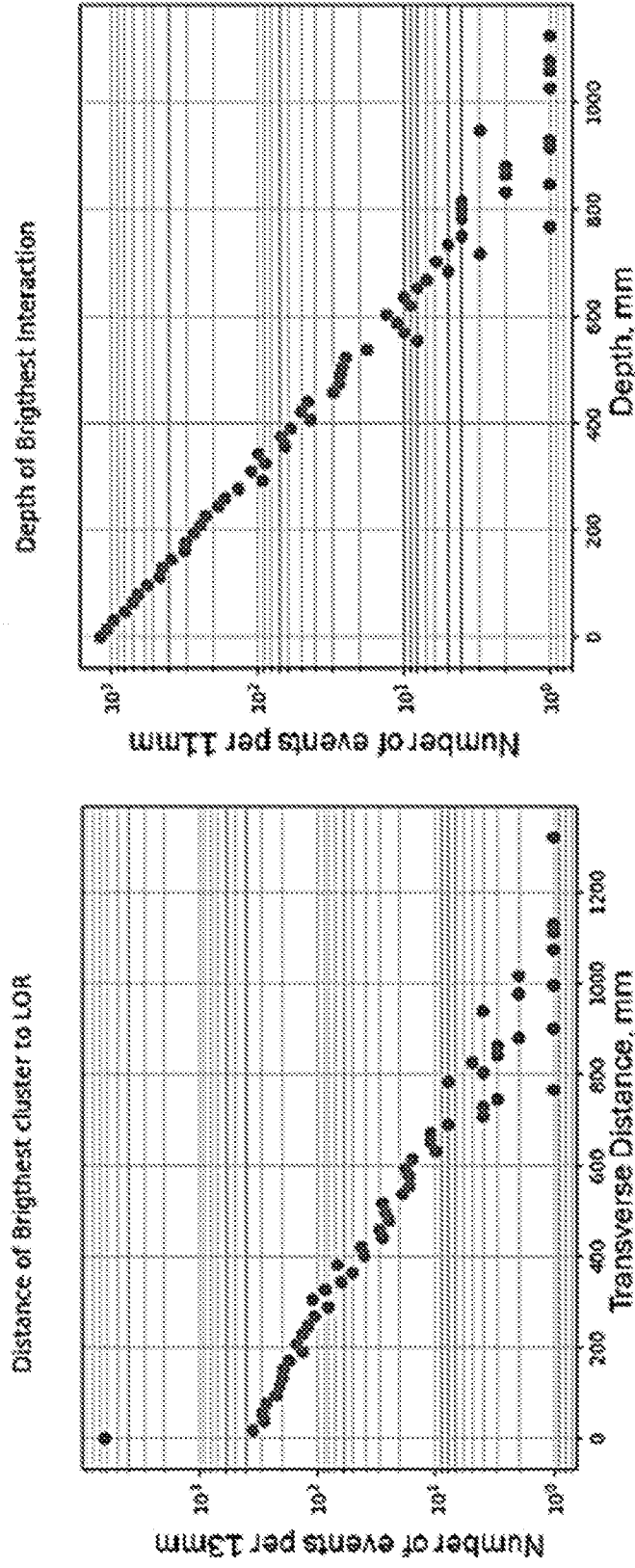Most energetic <u>energy</u> deposition

Distance of Brightest cluster to LOR

Depth of Brightest interaction

All annihilations									
4998									
Both Gammas interact most energetically in each's first interaction			One Gamma interacts most energetically in its first interaction			No Gammas interact most energetically in each's first interaction			
1697			2413			888			
Correct Electron End Reconstruction	One Incorrect Electron End Reconstruction	Two Incorrect Electron End Reconstructions	Correct Electron End Reconstruction	One Incorrect Electron End Reconstruction	Two Incorrect Electron End Reconstructions	Correct Electron End Reconstruction	One Incorrect Electron End Reconstruction	Two Incorrect Electron End Reconstructions	
1624	72	1	2207	204	2	778	103	7	

Events/0.002mm — Impact Parameter (mm)
Assumed Voxel Size, 20um

Events/9.4mm — Impact Parameter (mm)
Number of event median at 35 mm

Events/7.2mm — Impact Parameter (mm)
Peak at 30mm

FIG. 10

FIG. 11

Inset of first interaction

Recoil electron $E[\alpha]$

$\alpha[\text{rad}]$

$q[\text{keV}]$

Recoil gamma

True gamma
Line of response

True annihilation point

Opposing detector

FIG. 12

Inset of first interaction

Recoil electron
$E[e_0]$

$\theta[e_0]$

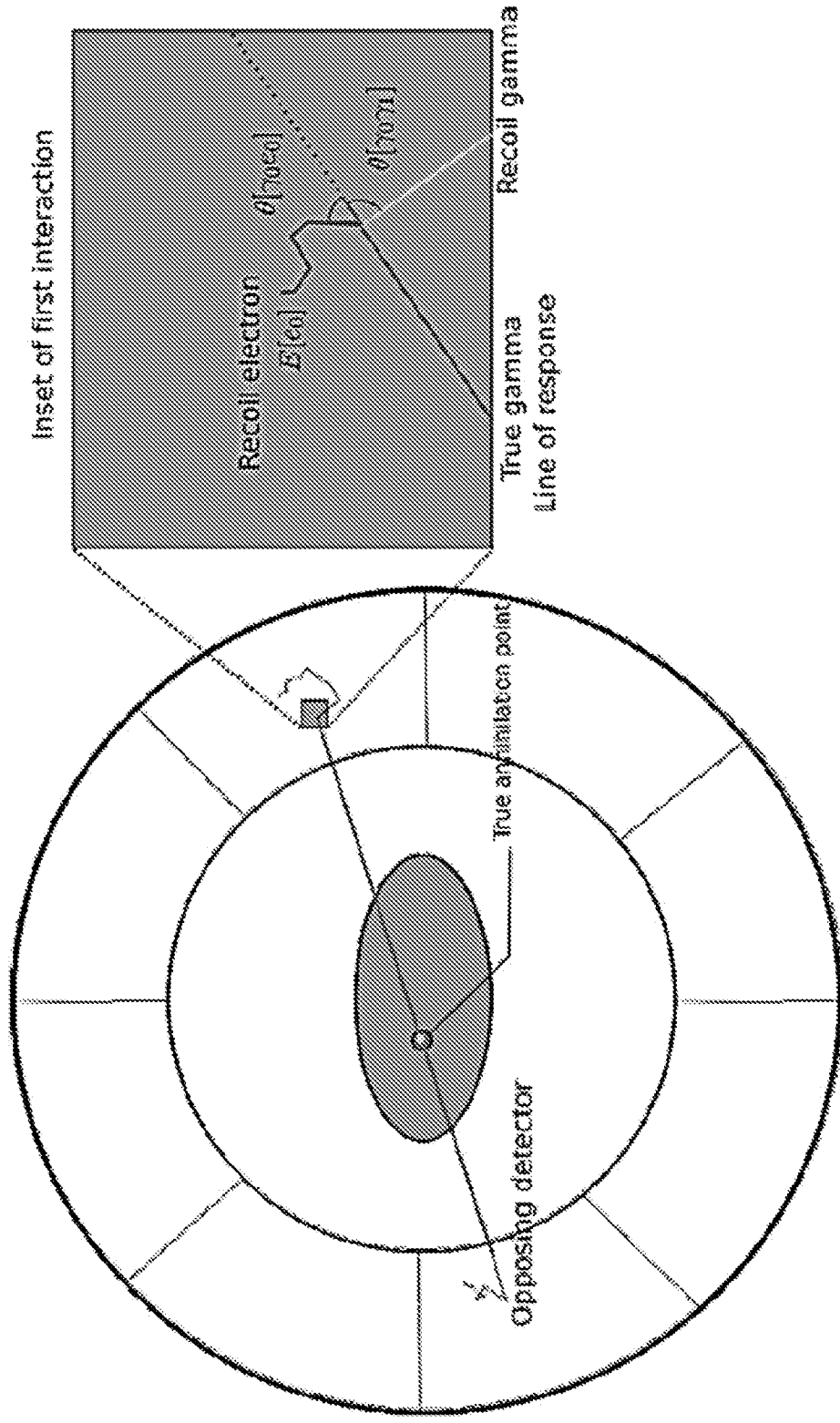$\theta[\gamma_0\gamma_1]$

True gamma

Recoil gamma

Line of response
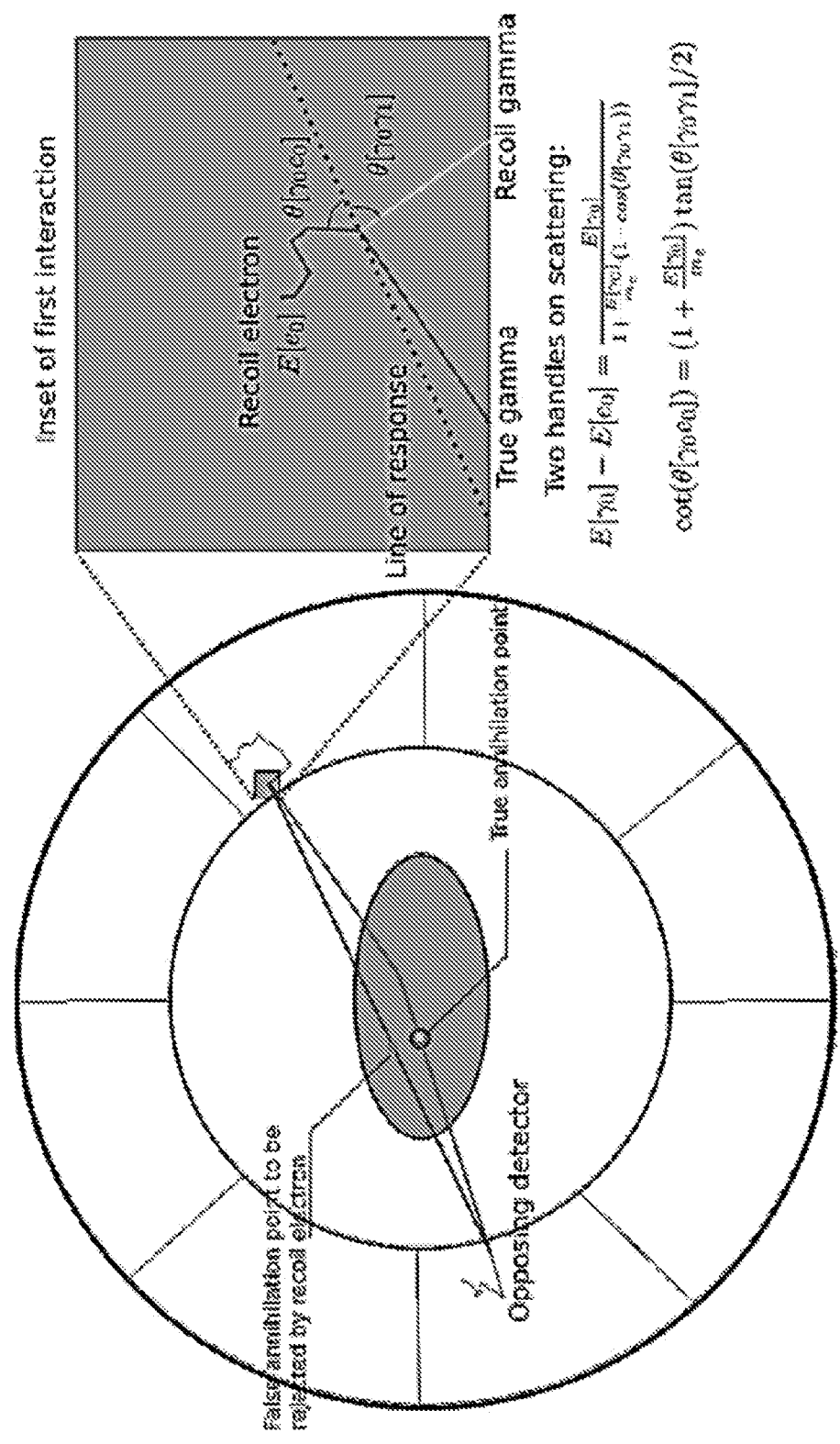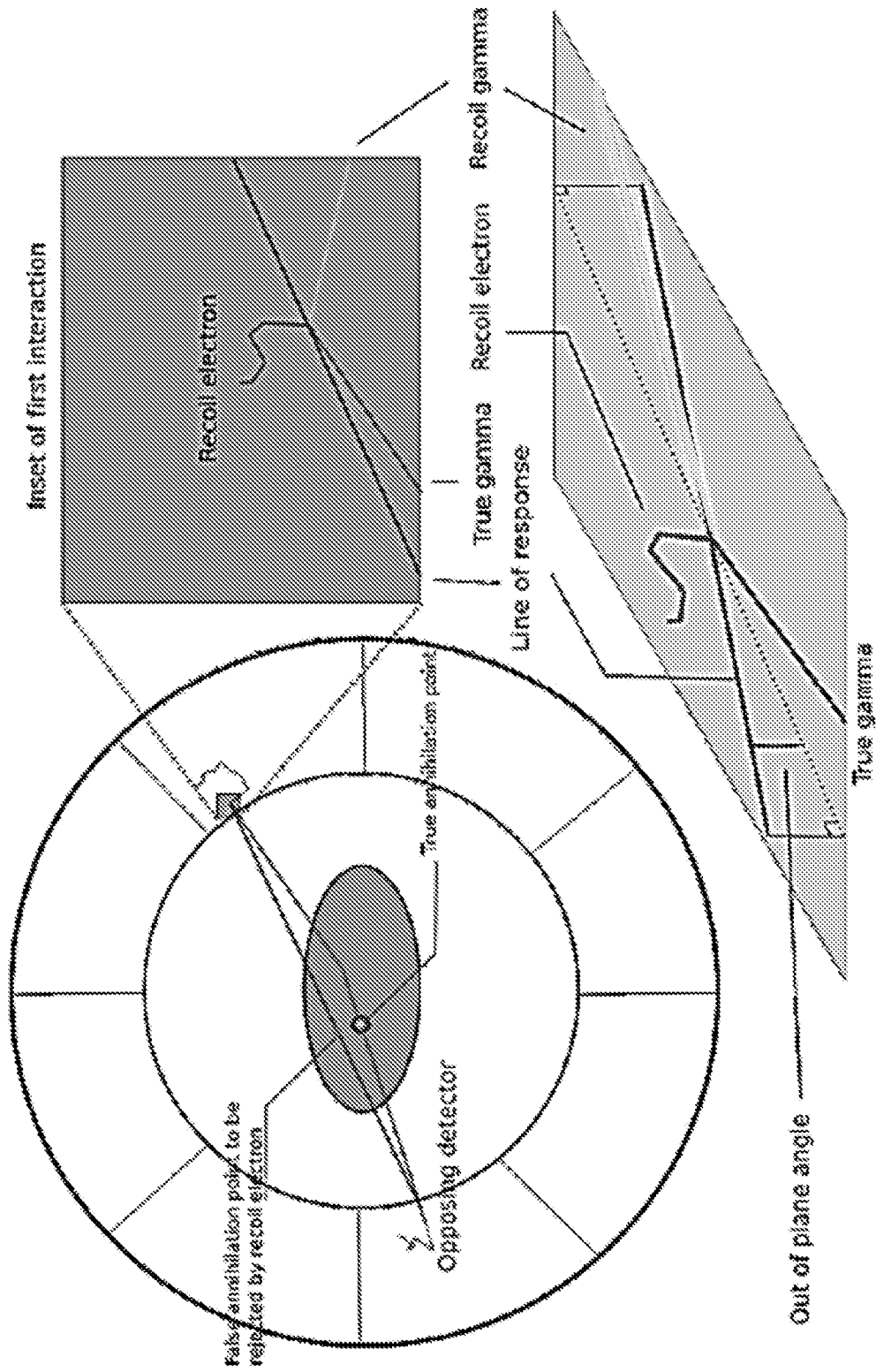
Two handles on scattering:

$$E[\gamma_0] - E[e_0] = \frac{E[\gamma_1]}{1 + \frac{E[\gamma_1]}{m_e}(1 - \cos(\theta[\gamma_0\gamma_1]))}$$

$$\cot(\theta[\gamma_0\gamma_1]) = \left(1 + \frac{E[\gamma_1]}{m_e}\right)\tan(\theta[\gamma_0\gamma_1]/2)$$

True annihilation point

Opposing detector

False annihilation point to be rejected by recoil electron

FIG. 13

Inset of first interaction

Recoil electron

True gamma

Line of response

Recoil gamma

Recoil electron

True gamma

False annihilation point to be rejected by recoil electron
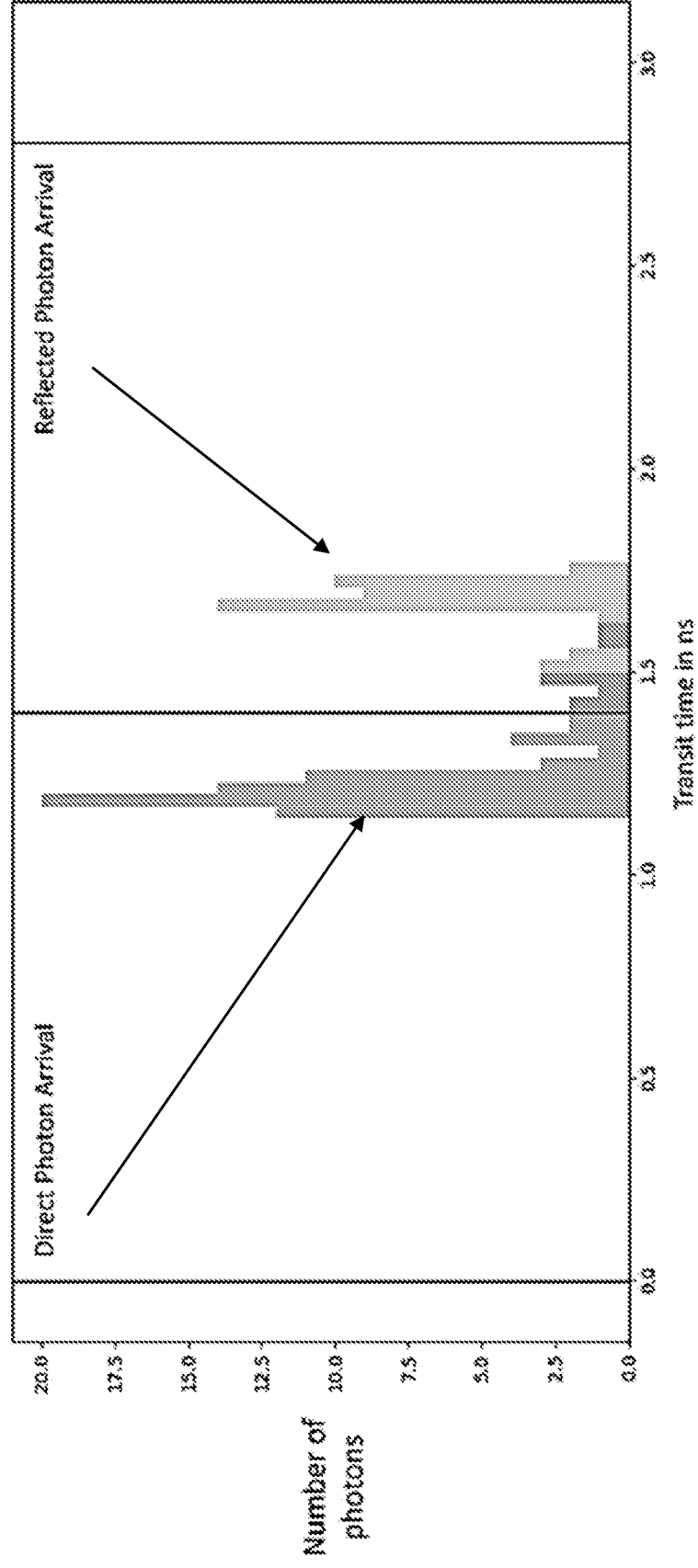
True annihilation point

Opposing detector

Out of plane angle

The recoil electron and recoil gamma momenta define a plane. If the line of response does not lie in this plane then there must have been a scatter before the detector.
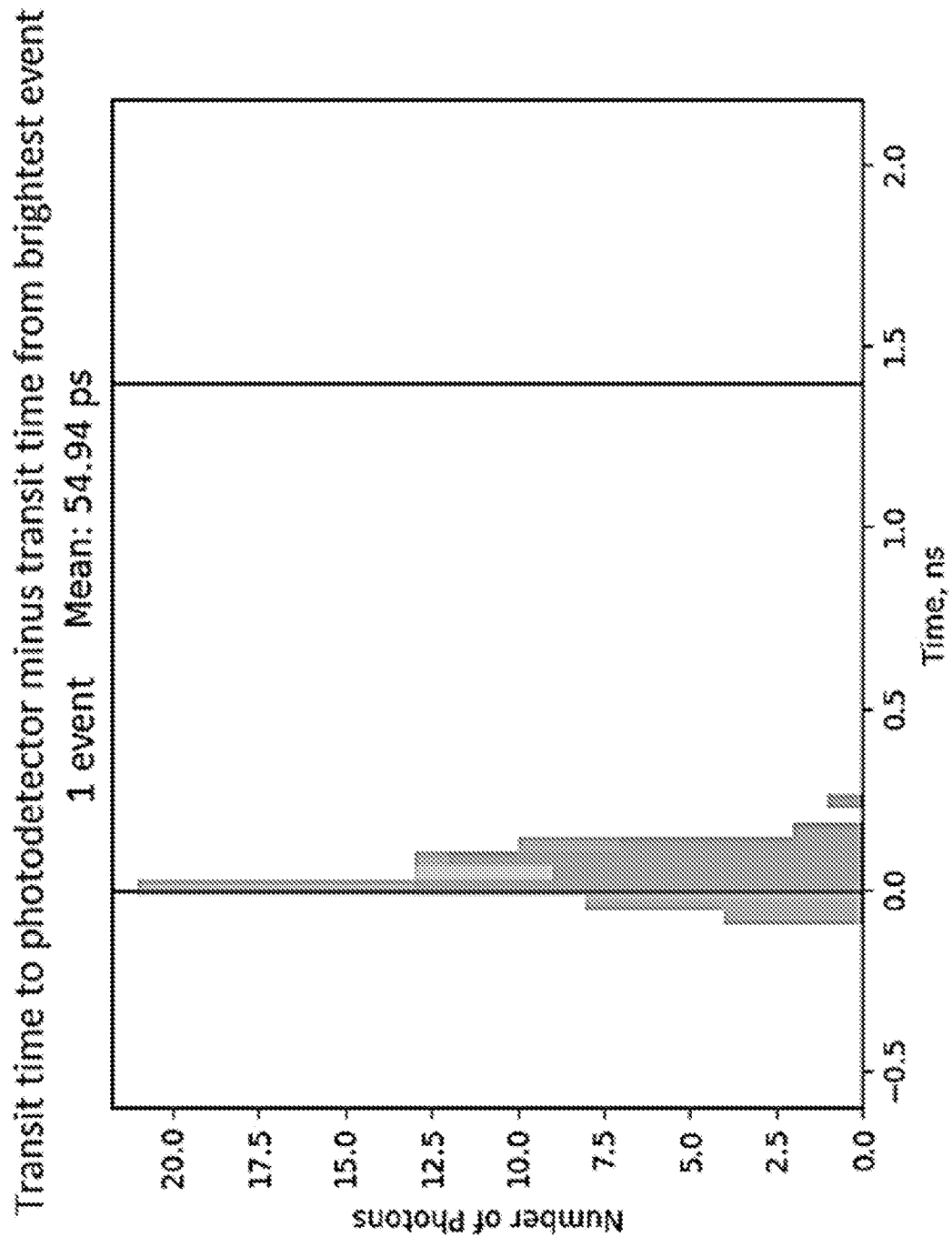
FIG. 14

Transit time of photons to rectangular photodetector directly and reflected.

Direct Photon Arrival

Reflected Photon Arrival

Number of photons

Transit time in ns

Section: Timing resolution

FIG. 15

Transit time to photodetector minus transit time from brightest event

1 event   Mean: 54.94 ps

Section: Timing resolution

FIG. 16

Time of Flight resolution for an infinitely fast scintillator given a point source on the main axis of the detector.
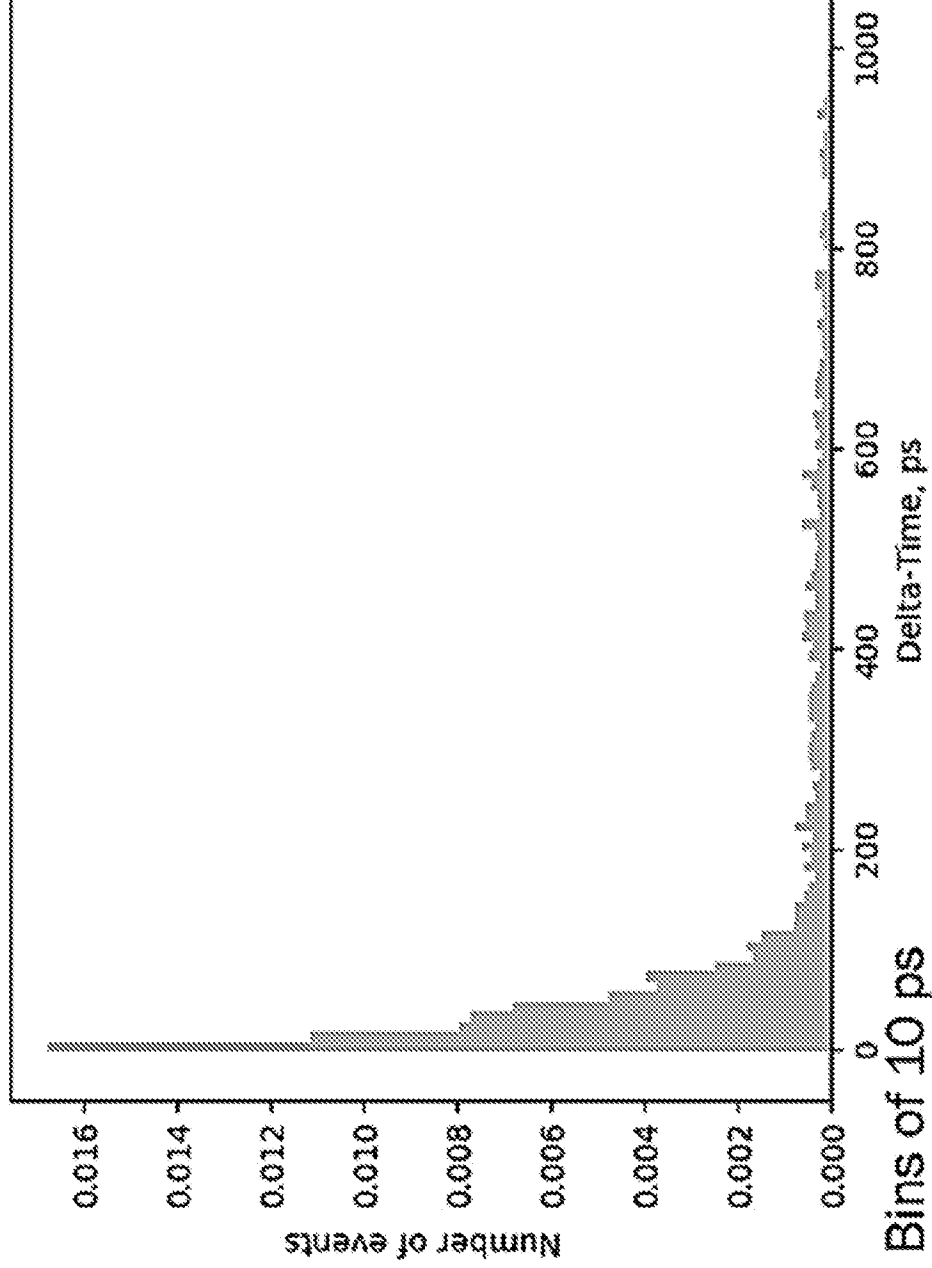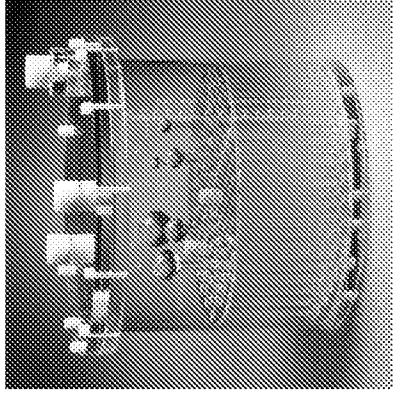
FIG. 17

Standard Jaszczak Phantom™
Model ECT/STD/P (Biodex 043-762)

For use with medium to high spatial resolution SPECT and PET systems.

Specifications:
Rod Height: 8.8 cm
Rod diameters: 6.4, 7.9, 9.5, 11.1, 12.7 and 19.1 mm
Solid sphere diameters: 12.7, 15.9, 19.1, 25.4, 31.8, and 38 mm
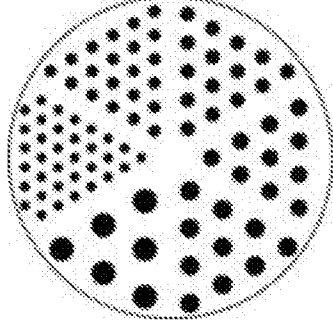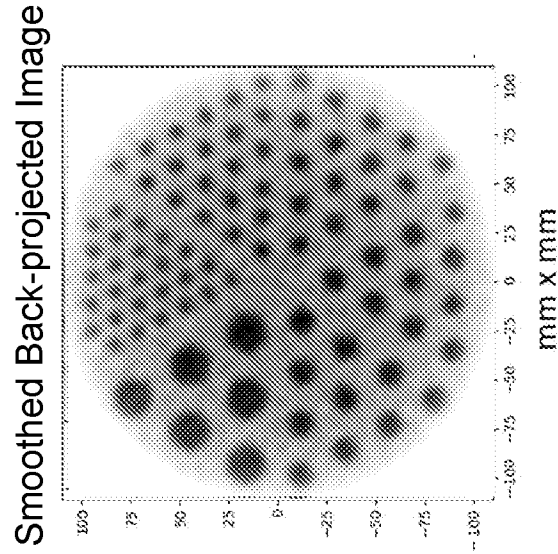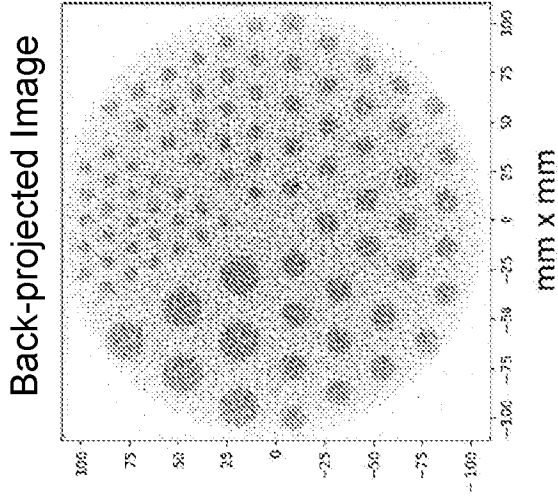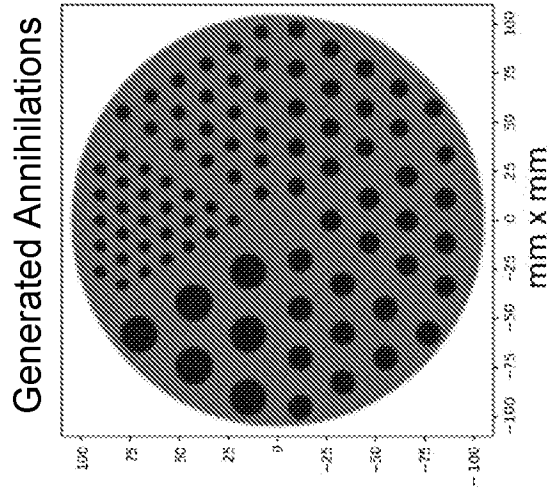Interior diameter: 21.6 cm

FIG. 18

100x DOSE REDUCTION

Generated Annihilations

mm x mm

Back-projected Image

mm x mm

Smoothed Back-projected Image

mm x mm

POWER OF ATTORNEY BY APPLICANT

I hereby revoke all previous powers of attorney given in the application identified in <u>either</u> the attached transmittal letter or the boxes below.

Application Number	Filing Date

(Note: The boxes above may be left blank if information is provided on form PTO/AIA/82A.)

[✓] I hereby appoint the Patent Practitioner(s) associated with the following Customer Number as my/our attorney(s) or agent(s), and to transact all business in the United States Patent and Trademark Office connected therewith for the application referenced in the attached transmittal letter (form PTO/AIA/82A) or identified above:

96227

OR

[ ] I hereby appoint Practitioner(s) named in the attached list (form PTO/AIA/82C) as my/our attorney(s) or agent(s), and to transact all business in the United States Patent and Trademark Office connected therewith for the patent application referenced in the attached transmittal letter (form PTO/AIA/82A) or identified above. (Note: Complete form PTO/AIA/82C.)

Please recognize or change the correspondence address for the application identified in the attached transmittal letter or the boxes above to:

[✓] The address associated with the above-mentioned Customer Number

OR

[ ] The address associated with Customer Number:

OR

[ ] Firm or Individual Name	
Address	
City	State	Zip
Country	
Telephone	Email

I am the Applicant (if the Applicant is a juristic entity, list the Applicant name in the box):

[ ] Inventor or Joint Inventor (title not required below)

[ ] Legal Representative of a Deceased or Legally Incapacitated Inventor (title not required below)

[✓] Assignee or Person to Whom the Inventor is Under an Obligation to Assign (provide signer's title if applicant is a juristic entity)

[ ] Person Who Otherwise Shows Sufficient Proprietary Interest (e.g., a petition under 37 CFR 1.46(b)(2) was granted in the application or is concurrently being filed with this document) (provide signer's title if applicant is a juristic entity)

SIGNATURE of Applicant for Patent

The undersigned (whose title is supplied below) is authorized to act on behalf of the applicant (e.g., where the applicant is a juristic entity).

Signature		Date (Optional)	
Name	Eric Ginsburg		
Title	Interim Director, Technology Commercialization, The University of Chicago		

<u>NOTE:</u> Signature - This form must be signed by the applicant in accordance with 37 CFR 1.33. See 37 CFR 1.4 for signature requirements and certifications. If more than one applicant, use multiple forms.

[ ] Total of _____ forms are submitted.

Electronic Patent Application Fee Transmittal

Application Number:	
Filing Date:	
Title of Invention:	POSITRON EMISSION TOMOGRAPHY SYSTEMS BASED ON IONIZATION-ACTIVATED ORGANIC FLUOR MOLECULES
First Named Inventor/Applicant Name:	Henry J. Frisch
Filer:	Michelle Manning/Carmen McCommon
Attorney Docket Number:	05400-0047-PV

Filed as Small Entity

Filing Fees for   Provisional

Description	Fee Code	Quantity	Amount	Sub-Total in USD($)
Basic Filing:				
PROVISIONAL APPLICATION FILING FEE	2005	1	150	150
Pages:				
Claims:				
Miscellaneous-Filing:				
Petition:				
Patent-Appeals-and-Interference:				
Post-Allowance-and-Post-Issuance:				

Description	Fee Code	Quantity	Amount	Sub-Total in USD($)
Extension-of-Time:				
Miscellaneous:				
		Total in USD ($)		150

Application Data Sheet 37 CFR 1.76	Attorney Docket Number	05400-0047-PV
	Application Number	

Title of Invention	POSITRON EMISSION TOMOGRAPHY SYSTEMS BASED ON IONIZATION-ACTIVATED ORGANIC FLUOR MOLECULES

The application data sheet is part of the provisional or nonprovisional application for which it is being submitted. The following form contains the bibliographic data arranged in a format specified by the United States Patent and Trademark Office as outlined in 37 CFR 1.76.

This document may be completed electronically and submitted to the Office in electronic format using the Electronic Filing System (EFS) or the document may be printed and included in a paper filed application.

Secrecy Order 37 CFR 5.2:

☐ Portions or all of the application associated with this Application Data Sheet may fall under a Secrecy Order pursuant to 37 CFR 5.2 (Paper filers only. Applications that fall under Secrecy Order may not be filed electronically.)

Inventor Information:

Inventor 1

Legal Name

Prefix	Given Name	Middle Name	Family Name	Suffix
	Henry	J.	Frisch	

Residence Information (Select One)	◉ US Residency	◯ Non US Residency	◯ Active US Military Service	

City	Chicago	State/Province	IL	Country of Residence [i]	US

Mailing Address of Inventor:

Address 1	5636 S. Blackstone Avenue		
Address 2			
City	Chicago	State/Province	IL
Postal Code	60637	Country [i]	US

Inventor 2

Legal Name

Prefix	Given Name	Middle Name	Family Name	Suffix
	Evan		Angelico	

Residence Information (Select One)	◉ US Residency	◯ Non US Residency	◯ Active US Military Service	

City	San Marcos	State/Province	CA	Country of Residence [i]	US

Mailing Address of Inventor:

Address 1	1736 Victoria Way		
Address 2			
City	San Marcos	State/Province	CA
Postal Code	92069	Country [i]	US

Inventor 3

Legal Name

Prefix	Given Name	Middle Name	Family Name	Suffix
	Patrick	J.	La Riviere	

PTO/AIA/14 (08-15)
Approved for use through 04/30/2017. OMB 0651-0032
U.S. Patent and Trademark Office; U.S. DEPARTMENT OF COMMERCE
Under the Paperwork Reduction Act of 1995, no persons are required to respond to a collection of information unless it contains a valid OMB control number.

Application Data Sheet 37 CFR 1.76	Attorney Docket Number	05400-0047-PV
	Application Number	

Title of Invention	POSITRON EMISSION TOMOGRAPHY SYSTEMS BASED ON IONIZATION-ACTIVATED ORGANIC FLUOR MOLECULES

Residence Information (Select One)	◉ US Residency	○ Non US Residency	○ Active US Military Service

City	Chicago	**State/Province**	IL	**Country of Residence** ^{i}	US

Mailing Address of Inventor:

Address 1	5406 S. University Avenue
Address 2	

City	Chicago		**State/Province**	IL
Postal Code	60615	**Country** ^{i}	US	

Inventor   4

Legal Name

Prefix	Given Name	Middle Name	Family Name	Suffix
	Bernhard	W.	Adams	

Residence Information (Select One)	◉ US Residency	○ Non US Residency	○ Active US Military Service

City	Naperville	**State/Province**	IL	**Country of Residence** ^{i}	US

Mailing Address of Inventor:

Address 1	1312 Saint Croix Avenue
Address 2	

City	Naperville		**State/Province**	IL
Postal Code	60564	**Country** ^{i}	US	

Inventor   5

Legal Name

Prefix	Given Name	Middle Name	Family Name	Suffix
	Eric		Spieglan	

Residence Information (Select One)	◉ US Residency	○ Non US Residency	○ Active US Military Service

City	Lisle	**State/Province**	IL	**Country of Residence** ^{i}	US

Mailing Address of Inventor:

Address 1	2131 Tellis Lane
Address 2	

City	Lisle		**State/Province**	IL
Postal Code	60532	**Country** ^{i}	US	

Inventor   6

Legal Name

Prefix	Given Name	Middle Name	Family Name	Suffix
	Joao	F.	Shida	

PTO/AIA/14 (08-15)
Approved for use through 04/30/2017. OMB 0651-0032
U.S. Patent and Trademark Office; U.S. DEPARTMENT OF COMMERCE
Under the Paperwork Reduction Act of 1995, no persons are required to respond to a collection of information unless it contains a valid OMB control number.

| Application Data Sheet 37 CFR 1.76 | Attorney Docket Number | 05400-0047-PV |
| | Application Number | |

| Title of Invention | POSITRON EMISSION TOMOGRAPHY SYSTEMS BASED ON IONIZATION-ACTIVATED ORGANIC FLUOR MOLECULES |

Residence Information (Select One) ◯ US Residency   ⦿ Non US Residency   ◯ Active US Military Service

| City | San Paulo | Country of Residence i | | ES |

Mailing Address of Inventor:

Address 1	Avenida Jurema 986		
Address 2			
City	San Paulo	**State/Province**	OT
Postal Code	040-79002	**Country** i	ES

Inventor   7

Legal Name

Prefix	Given Name	Middle Name	Family Name	Suffix
	Andrey		Elagin	

Residence Information (Select One) ⦿ US Residency   ◯ Non US Residency   ◯ Active US Military Service

| City | Bolingbrook | State/Province | IL | Country of Residence i | US |

Mailing Address of Inventor:

Address 1	625 Forest Way		
Address 2			
City	Bolingbrook	**State/Province**	IL
Postal Code	60440	**Country** i	US

All Inventors Must Be Listed - Additional Inventor Information blocks may be generated within this form by selecting the **Add** button. | Add |

Correspondence Information:

Enter either Customer Number or complete the Correspondence Information section below.
For further information see 37 CFR 1.33(a).

☐ **An Address is being provided for the correspondence Information of this application.**

| **Customer Number** | 96227 | | |
| **Email Address** | docketing@bellmanning.com | Add Email | Remove Email |

Application Information:

Title of the Invention	POSITRON EMISSION TOMOGRAPHY SYSTEMS BASED ON IONIZATION-ACTIVATED ORGANIC FLUOR MOLECULES		
Attorney Docket Number	05400-0047-PV	**Small Entity Status Claimed**	☒
Application Type	Provisional		
Subject Matter	Utility		
Total Number of Drawing Sheets (if any)	18	**Suggested Figure for Publication (if any)**	

Application Data Sheet 37 CFR 1.76	Attorney Docket Number	05400-0047-PV
	Application Number	

Title of Invention	POSITRON EMISSION TOMOGRAPHY SYSTEMS BASED ON IONIZATION-ACTIVATED ORGANIC FLUOR MOLECULES

Filing By Reference:

Only complete this section when filing an application by reference under 35 U.S.C. 111(c) and 37 CFR 1.57(a). Do not complete this section if application papers including a specification and any drawings are being filed. Any domestic benefit or foreign priority information must be provided in the appropriate section(s) below (i.e., "Domestic Benefit/National Stage Information" and "Foreign Priority Information").

For the purposes of a filing date under 37 CFR 1.53(b), the description and any drawings of the present application are replaced by this reference to the previously filed application, subject to conditions and requirements of 37 CFR 1.57(a).

Application number of the previously filed application	Filing date (YYYY-MM-DD)	Intellectual Property Authority or Country

Publication Information:

☐	Request Early Publication (Fee required at time of Request 37 CFR 1.219)
☐	**Request Not to Publish.** I hereby request that the attached application not be published under 35 U.S.C. 122(b) and certify that the invention disclosed in the attached application **has not and will not** be the subject of an application filed in another country, or under a multilateral international agreement, that requires publication at eighteen months after filing.

Representative Information:

Representative information should be provided for all practitioners having a power of attorney in the application. Providing this information in the Application Data Sheet does not constitute a power of attorney in the application (see 37 CFR 1.32).
Either enter Customer Number or complete the Representative Name section below. If both sections are completed the customer Number will be used for the Representative Information during processing.

Please Select One:	⦿ Customer Number	◯ US Patent Practitioner	◯ Limited Recognition (37 CFR 11.9)

Customer Number	96227

Prefix	Given Name	Middle Name	Family Name	Suffix	Remove

Registration Number	

Prefix	Given Name	Middle Name	Family Name	Suffix	Remove

Registration Number	

Additional Representative Information blocks may be generated within this form by selecting the **Add** button.

PTO/AIA/14 (08-15)
Approved for use through 04/30/2017. OMB 0651-0032
U.S. Patent and Trademark Office; U.S. DEPARTMENT OF COMMERCE
Under the Paperwork Reduction Act of 1995, no persons are required to respond to a collection of information unless it contains a valid OMB control number.

| **Application Data Sheet 37 CFR 1.76** | Attorney Docket Number | 05400-0047-PV |
| | Application Number | |

| Title of Invention | POSITRON EMISSION TOMOGRAPHY SYSTEMS BASED ON IONIZATION-ACTIVATED ORGANIC FLUOR MOLECULES |

Domestic Benefit/National Stage Information:

This section allows for the applicant to either claim benefit under 35 U.S.C. 119(e), 120, 121, 365(c), or 386(c) or indicate National Stage entry from a PCT application. Providing benefit claim information in the Application Data Sheet constitutes the specific reference required by 35 U.S.C. 119(e) or 120, and 37 CFR 1.78.
When referring to the current application, please leave the "Application Number" field blank.

Prior Application Status			Remove
Application Number	Continuity Type	Prior Application Number	Filing or 371(c) Date (YYYY-MM-DD)

Additional Domestic Benefit/National Stage Data may be generated within this form by selecting the **Add** button.

Foreign Priority Information:

This section allows for the applicant to claim priority to a foreign application. Providing this information in the application data sheet constitutes the claim for priority as required by 35 U.S.C. 119(b) and 37 CFR 1.55. When priority is claimed to a foreign application that is eligible for retrieval under the priority document exchange program (PDX) the information will be used by the Office to automatically attempt retrieval pursuant to 37 CFR 1.55(i)(1) and (2). Under the PDX program, applicant bears the ultimate responsibility for ensuring that a copy of the foreign application is received by the Office from the participating foreign intellectual property office, or a certified copy of the foreign priority application is filed, within the time period specified in 37 CFR 1.55(g)(1).

Application Number	Country[i]	Filing Date (YYYY-MM-DD)	Access Code[i] (if applicable)

Additional Foreign Priority Data may be generated within this form by selecting the **Add** button.

Statement under 37 CFR 1.55 or 1.78 for AIA (First Inventor to File) Transition Applications

| ☐ | This application (1) claims priority to or the benefit of an application filed before March 16, 2013 and (2) also contains, or contained at any time, a claim to a claimed invention that has an effective filing date on or after March 16, 2013.
NOTE: By providing this statement under 37 CFR 1.55 or 1.78, this application, with a filing date on or after March 16, 2013, will be examined under the first inventor to file provisions of the AIA. |

| **Application Data Sheet 37 CFR 1.76** | Attorney Docket Number | 05400-0047-PV |
| | Application Number | |

| Title of Invention | POSITRON EMISSION TOMOGRAPHY SYSTEMS BASED ON IONIZATION-ACTIVATED ORGANIC FLUOR MOLECULES |

Authorization or Opt-Out of Authorization to Permit Access:

When this Application Data Sheet is properly signed and filed with the application, applicant has provided written authority to permit a participating foreign intellectual property (IP) office access to the instant application-as-filed (see paragraph A in subsection 1 below) and the European Patent Office (EPO) access to any search results from the instant application (see paragraph B in subsection 1 below).

Should applicant choose not to provide an authorization identified in subsection 1 below, applicant **must opt-out** of the authorization by checking the corresponding box A or B or both in subsection 2 below.

NOTE: This section of the Application Data Sheet is **ONLY** reviewed and processed with the **INITIAL** filing of an application. After the initial filing of an application, an Application Data Sheet cannot be used to provide or rescind authorization for access by a foreign IP office(s). Instead, Form PTO/SB/39 or PTO/SB/69 must be used as appropriate.

1. Authorization to Permit Access by a Foreign Intellectual Property Office(s)

A. Priority Document Exchange (PDX) - Unless box A in subsection 2 (opt-out of authorization) is checked, the undersigned hereby **grants the USPTO authority** to provide the European Patent Office (EPO), the Japan Patent Office (JPO), the Korean Intellectual Property Office (KIPO), the State Intellectual Property Office of the People's Republic of China (SIPO), the World Intellectual Property Organization (WIPO), and any other foreign intellectual property office participating with the USPTO in a bilateral or multilateral priority document exchange agreement in which a foreign application claiming priority to the instant patent application is filed, access to: (1) the instant patent application-as-filed and its related bibliographic data, (2) any foreign or domestic application to which priority or benefit is claimed by the instant application and its related bibliographic data, and (3) the date of filing of this Authorization. See 37 CFR 1.14(h)(1).

B. Search Results from U.S. Application to EPO - Unless box B in subsection 2 (opt-out of authorization) is checked, the undersigned hereby **grants the USPTO authority** to provide the EPO access to the bibliographic data and search results from the instant patent application when a European patent application claiming priority to the instant patent application is filed. See 37 CFR 1.14(h)(2).

The applicant is reminded that the EPO's Rule 141(1) EPC (European Patent Convention) requires applicants to submit a copy of search results from the instant application without delay in a European patent application that claims priority to the instant application.

2. Opt-Out of Authorizations to Permit Access by a Foreign Intellectual Property Office(s)

☐ A. Applicant **DOES NOT** authorize the USPTO to permit a participating foreign IP office access to the instant application-as-filed. If this box is checked, the USPTO will not be providing a participating foreign IP office with any documents and information identified in subsection 1A above.

☐ B. Applicant **DOES NOT** authorize the USPTO to transmit to the EPO any search results from the instant patent application. If this box is checked, the USPTO will not be providing the EPO with search results from the instant application.

NOTE: Once the application has published or is otherwise publicly available, the USPTO may provide access to the application in accordance with 37 CFR 1.14.

Application Data Sheet 37 CFR 1.76	Attorney Docket Number	05400-0047-PV
	Application Number	

Title of Invention	POSITRON EMISSION TOMOGRAPHY SYSTEMS BASED ON IONIZATION-ACTIVATED ORGANIC FLUOR MOLECULES

Applicant Information:

Providing assignment information in this section does not substitute for compliance with any requirement of part 3 of Title 37 of CFR to have an assignment recorded by the Office.

Applicant   1

If the applicant is the inventor (or the remaining joint inventor or inventors under 37 CFR 1.45), this section should not be completed. The information to be provided in this section is the name and address of the legal representative who is the applicant under 37 CFR 1.43; or the name and address of the assignee, person to whom the inventor is under an obligation to assign the invention, or person who otherwise shows sufficient proprietary interest in the matter who is the applicant under 37 CFR 1.46. If the applicant is an applicant under 37 CFR 1.46 (assignee, person to whom the inventor is obligated to assign, or person who otherwise shows sufficient proprietary interest) together with one or more joint inventors, then the joint inventor or inventors who are also the applicant should be identified in this section.

	Clear

○ Assignee	○ Legal Representative under 35 U.S.C. 117	○ Joint Inventor

⦿ Person to whom the inventor is obligated to assign.	○ Person who shows sufficient proprietary interest

If applicant is the legal representative, indicate the authority to file the patent application, the inventor is:

Name of the Deceased or Legally Incapacitated Inventor:	

If the Applicant is an Organization check here.	☒

Organization Name	The University of Chicago

Mailing Address Information For Applicant:

Address 1	5801 S. Ellis Avenue		
Address 2			
City	Chicago	**State/Province**	IL
Country[i]	US	Postal Code	60637
Phone Number		Fax Number	
Email Address			

Additional Applicant Data may be generated within this form by selecting the Add button.

| **Application Data Sheet 37 CFR 1.76** | Attorney Docket Number | 05400-0047-PV |
| | Application Number | |

| Title of Invention | POSITRON EMISSION TOMOGRAPHY SYSTEMS BASED ON IONIZATION-ACTIVATED ORGANIC FLUOR MOLECULES |

Assignee Information including Non-Applicant Assignee Information:

Providing assignment information in this section does not substitute for compliance with any requirement of part 3 of Title 37 of CFR to have an assignment recorded by the Office.

Assignee   1
Complete this section if assignee information, including non-applicant assignee information, is desired to be included on the patent application publication. An assignee-applicant identified in the "Applicant Information" section will appear on the patent application publication as an applicant. For an assignee-applicant, complete this section only if identification as an assignee is also desired on the patent application publication.

If the Assignee or Non-Applicant Assignee is an Organization check here.			☐	
Prefix	**Given Name**	Middle Name	**Family Name**	Suffix

Mailing Address Information For Assignee including Non-Applicant Assignee:

Address 1	
Address 2	

City		**State/Province**	
Country i		Postal Code	
Phone Number		Fax Number	
Email Address			

Additional Assignee or Non-Applicant Assignee Data may be generated within this form by selecting the Add button.

PTO/AIA/14 (08-15)
Approved for use through 04/30/2017. OMB 0651-0032
U.S. Patent and Trademark Office; U.S. DEPARTMENT OF COMMERCE
Under the Paperwork Reduction Act of 1995, no persons are required to respond to a collection of information unless it contains a valid OMB control number.

| **Application Data Sheet 37 CFR 1.76** | Attorney Docket Number | 05400-0047-PV |
| | Application Number | |

| Title of Invention | POSITRON EMISSION TOMOGRAPHY SYSTEMS BASED ON IONIZATION-ACTIVATED ORGANIC FLUOR MOLECULES |

Signature:

NOTE: This Application Data Sheet must be signed in accordance with 37 CFR 1.33(b). **However, if this Application Data Sheet is submitted with the <u>INITIAL</u> filing of the application <u>and</u> either box A or B is <u>not</u> checked in subsection 2 of the "Authorization or Opt-Out of Authorization to Permit Access" section, then this form must also be signed in accordance with 37 CFR 1.14(c).**

This Application Data Sheet **must** be signed by a patent practitioner if one or more of the applicants is a **juristic   entity** (e. g., corporation or association). If the applicant is two or more joint inventors, this form must be signed by a patent practitioner, **all** joint inventors who are the applicant, or one or more joint inventor-applicants who have been given power of attorney (e.g., see USPTO Form PTO/AIA/81) on behalf of **all** joint inventor-applicants.

See 37 CFR 1.4(d) for the manner of making signatures and certifications.

Signature	/Michelle Manning/			Date (YYYY-MM-DD)	
First Name	Michelle	**Last Name**	Manning	**Registration Number**	50592
Additional Signature may be generated within this form by selecting the Add button.					